Research Square

Preprints are preliminary reports that have not undergone peer review.
They should not be considered conclusive, used to inform clinical practice,
or referenced by the media as validated information.

Decoupled geogenic and faecal hazards in shallow coastal groundwater: evidence and a screening framework from the lower Indus Delta, Pakistan

Tarique Mahmood Noonari
Pakistan Council of Research in Water Resources
Nadeem Gul
nadeem.gul@stu.xidian.edu.cn
Xidian University
Ms Sawera
Shah Abdul Latif University
Ms Yousra
Sukkur IBA University

Research Article

Keywords: Coastal aquifer, Seawater intrusion, Faecal contamination, Entropy water quality index, Monte Carlo health risk, Hazard typology

Posted Date: November 4th, 2026

DOI: https://doi.org/10.21203/rs.3.rs-11325464/v1

License: This work is licensed under a Creative Commons Attribution 4.0 International License.
Read Full License

Additional Declarations: No competing interests reported.

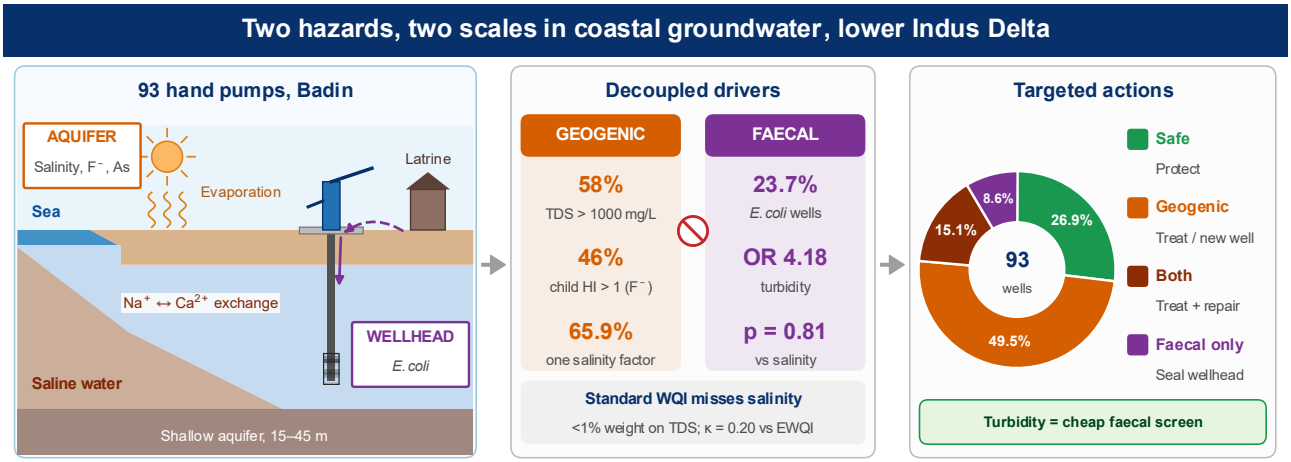
Decoupled geogenic and faecal hazards in shallow coastal groundwater: evidence and a screening framework from the lower Indus Delta, Pakistan

Tarique Mahmood Noonari[a], Nadeem Gul[b,*], Sawera[d], Yousra[e]

[a] *Pakistan Council of Research in Water Resources (PCRWR), Water Quality Laboratory, Badin, Sindh, Pakistan*
[b] *School of Optoelectronics Engineering, Xidian University, Xi'an 710071, China*
[d] *Department of Botany, Shah Abdul Latif University, Khairpur, Pakistan*
[e] *Department of Computer Science, Sukkur IBA University, Kandhkot Campus, Kandhkot, Pakistan*

[*] Corresponding author: Nadeem Gul (nadeem.gul@stu.xidian.edu.cn)

Graphical abstract



Separate hazards by origin and scale for targeted, affordable interventions

Highlights

- Only 27% of 93 hand pumps were free of salinity, fluoride, arsenic and *E. coli*
- Salinity arises from evaporation, cation exchange and limited marine mixing
- *E. coli* was independent of salinity and tracked turbidity, pointing to wellhead entry
- Conventional WQI agreed poorly with entropy WQI (weighted $\kappa = 0.20$)
- Monte Carlo hazard index exceeded 1 in 46% of child exposures, driven by fluoride

Abstract

Shallow hand pumps supply drinking water to millions of people in low-lying deltas worldwide, where groundwater is exposed to geogenic salinisation and faecal contamination. Because these hazards are usually assessed together, it remains unclear whether they share a pathway and, therefore, which interventions are needed. In the lower Indus Delta (Pakistan), we analysed 93 hand pumps for 16 physicochemical variables, total coliforms and *Escherichia coli*, and combined hydrochemical diagnostics, a seawater mixing index (SMI), multivariate statistics, entropy-weighted and weighted-arithmetic water quality indices (EWQI, WA-WQI) and deterministic and Monte Carlo health-risk models. TDS exceeded 1000 mg/L in 58.1% of wells. A single salinity factor (65.9% of variance) integrated evaporation, cation exchange (slope −0.95, $R^2 = 0.97$) and limited marine mixing (SMI > 1 in 23.7%). *E. coli* occurred in 23.7% of wells, was independent of salinity (OR = 0.83, p = 0.81), was predicted only by turbidity (OR = 4.18 per $\log_{10}$ NTU; AUC = 0.82) and, unlike salinity, was not spatially clustered, indicating wellhead ingress. WA-WQI assigned 66% of its weight to F^- and turbidity and agreed poorly with EWQI (weighted $\kappa = 0.20$). Child hazard index exceeded 1 with 46.1% probability, driven by F^-, and drinking water supplied

up to 122% of the WHO daily sodium limit. A well-by-well typology showed that only 26.9% of wells were safe, 8.6% needed only wellhead repair and 64.6% required treatment or a new source. The framework uses only routine monitoring data and is transferable to other salinising coastal deltas.

Keywords: Coastal aquifer; Seawater intrusion; Faecal contamination; Entropy water quality index; Monte Carlo health risk; Hazard typology

1. Introduction

1.1 Coastal groundwater under pressure

Shallow coastal aquifers supply drinking water to a large part of the world's population, yet they are among the most fragile groundwater systems because fresh water floats on, and is bounded by, denser saline water (Werner et al., 2013). Their vulnerability is controlled mainly by human pressure: intensive pumping and reduced river inflow can move the freshwater–saltwater interface landward faster than sea-level rise alone (Ferguson & Gleeson, 2012), although rising seas are projected to expand the populations drinking saline groundwater by 2050 (Mueller et al., 2024). Large deltas are especially exposed because sediment starvation and compaction make them subside while upstream abstraction lowers the hydraulic head that once kept marine water offshore (Syvitski et al., 2009). Recent work on the coasts of South Asia shows how pervasive the outcome is. More than half of 1228 wells on the east coast of India carry a seawater-mixing signature (Sarkar et al., 2026), and ion exchange, seawater mixing and abstraction jointly govern salinisation in the coastal aquifers of eastern and western India (Agarwal & Dhakate, 2024; Goswami & Rai, 2025; Sarkar et al., 2026).

1.2 Health relevance of geogenic and microbial hazards

Salinised drinking water is a health concern as well as a taste problem. In coastal Bangladesh, drinking-water salinity has been associated with hypertensive disorders of pregnancy and with raised blood pressure in adults (Khan et al., 2011; Scheelbeek et al., 2017; Naser et al., 2019), and the number of people exposed to saline drinking water is expected to rise under 2050 climate scenarios (Mueller et al., 2024). The young alluvial aquifers of the Indus and Ganges basins also carry geogenic arsenic and fluoride (Podgorski et al., 2017; Podgorski & Berg, 2020; Ullah et al., 2026), while agricultural nitrate adds a further chronic exposure (Ward et al., 2018). In addition,

faecal indicator bacteria are frequently detected in sources classed as improved in low- and middle-income countries (Bain et al., 2014), and unsafe water remains a major cause of diarrhoeal disease (Prüss-Ustün et al., 2019).

These hazards differ in origin and therefore in remedy. Salinity, hardness, fluoride and arsenic are acquired from the aquifer, vary over kilometres and require desalination, defluoridation or an alternative source. Faecal contamination often enters at the well itself. Studies in the shallow aquifers of Bangladesh have shown that unsealed annuli allow rapid downward flow of contaminated water (Knappett et al., 2012), that hand pumps can harbour *E. coli* (Ferguson et al., 2011), and that faecal contamination of shallow tubewells can be unrelated, or even inversely related, to aquifer chemistry (van Geen et al., 2011). Pit latrines contribute mainly where they are close to wells and the unsaturated zone is thin (Bagordo et al., 2024), contamination rises in the wet season (Kostyla et al., 2015), and sanitary-inspection scores are poor predictors of *E. coli* in tubewells (Ercumen et al., 2017). Separating aquifer-scale from wellhead-scale contamination is therefore essential for choosing interventions that work.

1.3 The lower Indus Delta and District Badin

Groundwater has become the backbone of irrigation and domestic supply in Pakistan, but its governance has lagged far behind abstraction (Qureshi, 2020), and national reviews consistently report bacteriological, physicochemical and toxic-element failures in drinking water (Fida et al., 2023). The lower Indus Delta in southern Sindh is the most acute case. Diminished river and sediment discharge has turned the delta front into an eroding, wave-dominated coast (Giosan et al., 2006), and multi-decadal satellite analysis documents continuing shoreline retreat, mangrove loss and saline encroachment (Aeman et al., 2023). Groundwater in coastal Badin, Sindh, is largely unsuitable for drinking because of salinity (Alamgir et al., 2016), and index-based surveys in the Indus Delta and Sujawal have classed large shares of wells as poor to unsuitable (Solangi et al., 2019a, 2020). Fluoride enrichment has been reported in the unconfined aquifer of Badin (Talpur et al., 2020) and in community tube wells elsewhere in Sindh (Ullah et al., 2025), and chemical and bacteriological failures have both been recorded in Badin drinking water (Ali et al., 2024).

1.4 Methodological gaps and objectives

Two methodological weaknesses limit how far existing studies can guide management. First, most regional assessments rely on the weighted-arithmetic water quality index (WA-WQI; Brown et al., 1970), in which the weight of each parameter is inversely proportional to its guideline value. Reviews of index models have warned that weighting and aggregation choices can cause eclipsing

and misleading classifications (Uddin et al., 2021), but the behaviour of WA-WQI in saline aquifers has not been tested against a data-driven benchmark. Entropy-weighted indices (EWQI) weight each variable by its information content (Li et al., 2010; Amiri et al., 2014) and are now commonly paired with probabilistic health-risk assessment (Raicy et al., 2026; Yadav & Kalkal, 2024; Du et al., 2025). Second, chemical and microbiological results are usually reported side by side rather than tested against each other. Whether faecal contamination shares the origin and spatial scale of the chemical hazards is therefore assumed rather than demonstrated, even though the answer determines whether a well needs a new source, a treatment unit or simply a repaired apron.

We propose that drinking-water risk in deltaic coastal aquifers is best understood as two decoupled hazards acting at two scales: an aquifer-scale geogenic hazard (salinity, fluoride, arsenic) and a wellhead-scale faecal hazard. We test this 'two hazards, two scales' hypothesis for 93 drinking-water hand pumps in the Badin and Shaheed Fazul Rahoo talukas. The objectives were to: (1) characterise groundwater chemistry and guideline compliance; (2) identify and rank the processes responsible for salinisation; (3) benchmark WA-WQI against EWQI and diagnose the source of their disagreement; (4) test whether faecal indicators are linked to aquifer chemistry or to wellhead condition; (5) quantify deterministic and Monte Carlo health risks for adults and children; and (6) translate these results into a well-by-well hazard typology that assigns each source to an intervention class.

This work makes three contributions. First, to our knowledge, it is the first study in the lower Indus Delta to test statistically, on the same wells, whether faecal contamination shares the origin and spatial scale of the geogenic hazards, instead of reporting the two side by side. Second, it benchmarks the weighted-arithmetic WQI, which underpins almost all previous assessments of coastal Sindh, against an entropy-weighted index and isolates the single parameter responsible for their disagreement. Third, it converts hydrochemical, microbiological and probabilistic risk results into a well-by-well hazard typology that assigns each source to an intervention class, providing a transferable decision tool for low-income coastal deltas where monitoring budgets are limited.

2. Study area

2.1 Location and setting

The study covers three union councils (UCs) of District Badin, southern Sindh: Gharo in Taluka Shaheed Fazul Rahoo, and Kadi Kazia and Sirani in Taluka Badin (Fig. 1). The sampled wells lie between 24°26′ and 24°47′ N and between 68°40′ and 68°51′ E on the eastern flank of the lower Indus Delta, inland of the Arabian Sea coast; Sirani is the southernmost and most coastal of the

three UCs. The 93 sampling points serve 54 villages in which piped supply is absent or intermittent and households rely on private or communal hand pumps.

The climate is arid to semi-arid. Summers are very hot, rainfall is low and erratic and falls mostly during the July–September monsoon, and potential evaporation greatly exceeds precipitation. The terrain is a flat, low-lying alluvial plain crossed by irrigation canals and by the Left Bank Outfall Drain system, which carries saline drainage effluent towards the coast.

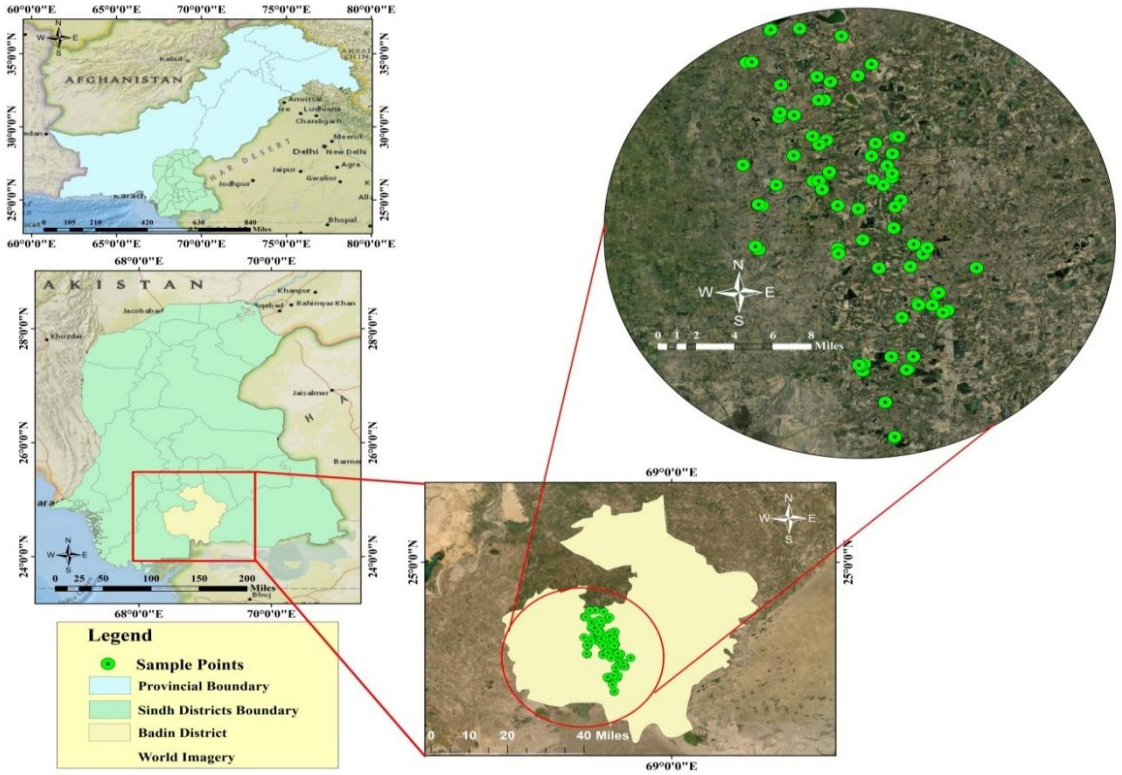


Fig. 1. Location of the study area and the sampled hand pumps/bore wells in Talukas Badin and Shaheed Fazul Rahoo, District Badin, Sindh, Pakistan.

2.2 Geology and hydrogeology

District Badin lies in the Lower Indus Basin on the south-western margin of the Indian Plate. Mesozoic carbonates and clastics, including the Chiltan Limestone and the Sembar and Goru formations, occur at depth, but the land surface is covered almost entirely by unconsolidated Holocene deltaic and alluvial deposits of interbedded silt, fine sand and clay, with no significant outcrops (Fig. 2). The hand pumps tap the uppermost unconfined part of this sequence at depths of 15–45 m. This shallow aquifer is recharged mainly by canal seepage, irrigation return flow and monsoon infiltration, is chemically young and is highly heterogeneous at the scale of individual wells.

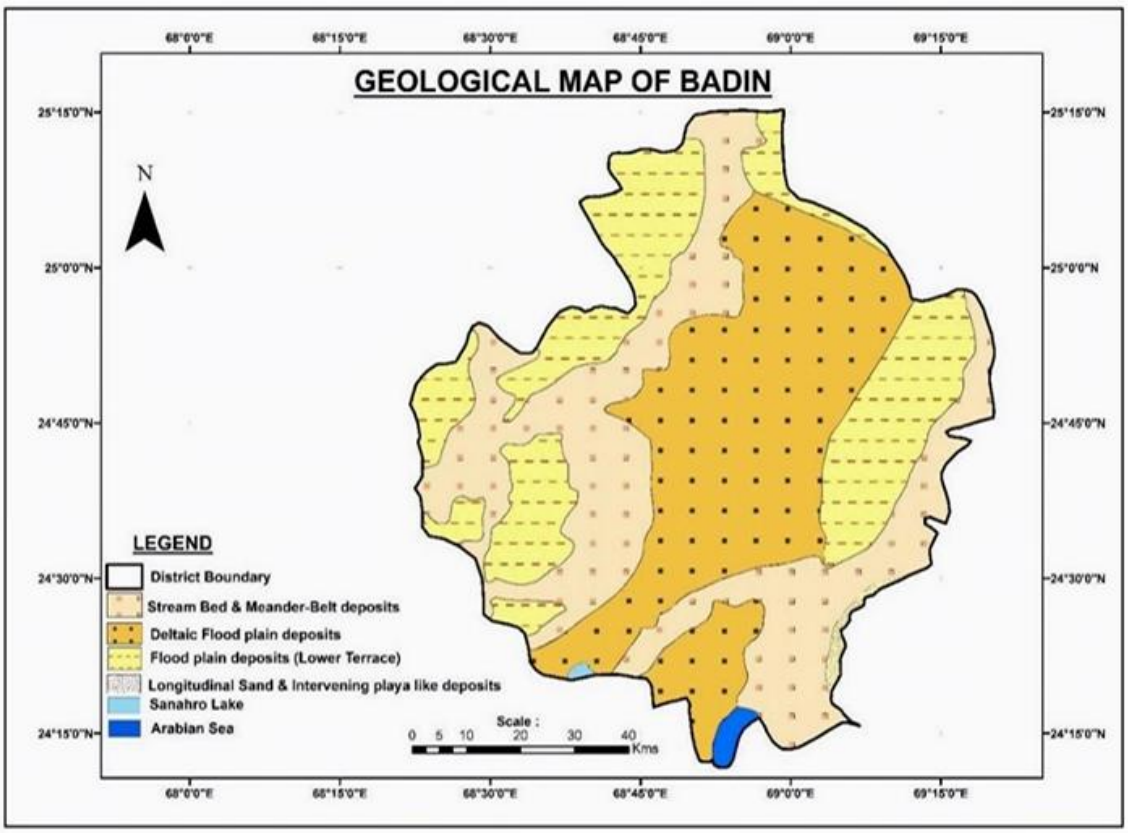


Fig. 2. Geological map of District Badin, Sindh, Pakistan.

3. Materials and methods

3.1 Field sampling

Ninety-three hand pumps were sampled (37 in Gharo, 29 in Kadi Kazia and 27 in Sirani; Fig. 3) during a single field campaign. Wells were selected to represent the sources actually used for drinking in each UC and to cover the settlement pattern. Depth (15–45 m; mean 24.1 ± 5.8 m) was obtained from owners and caretakers, and coordinates were recorded with a handheld GPS. Each pump was operated until the discharge ran clear before sampling. Water for physicochemical analysis was collected in pre-cleaned polyethylene bottles rinsed three times with sample water, water for nitrate in separate 200 mL containers and water for bacteriological analysis in sterilised bottles. Samples were labelled, kept cool and delivered to the Water Quality Laboratory of the Pakistan Council of Research in Water Resources (PCRWR), Badin.

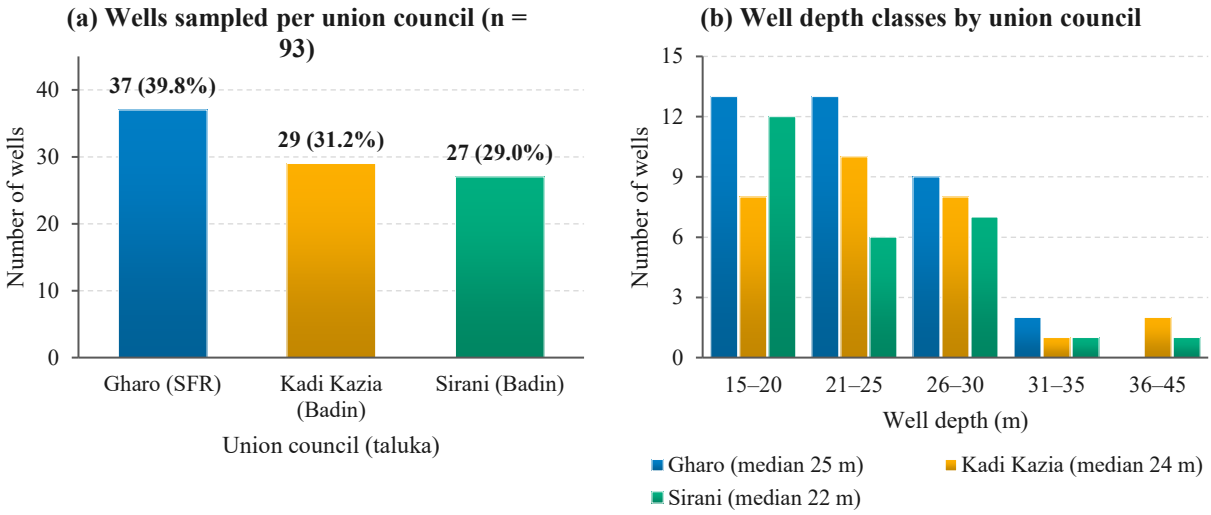


Fig. 3. Sampling design: (a) number (and share) of hand pumps sampled in each union council, Gharo (Taluka Shaheed Fazul Rahoo) and Kadi Kazia and Sirani (Taluka Badin); (b) distribution of well depths by union council.

3.2 Laboratory analysis and quality control

All determinations followed APHA (2012). pH, electrical conductivity (EC) and turbidity were measured with calibrated digital meters; total alkalinity and HCO_3^- by acid titration; Cl^- by argentometric titration; Ca^{2+} and Mg^{2+} by EDTA titration, with total hardness (TH) expressed as $CaCO_3$; SO_4^{2-} turbidimetrically; and Na^+ and K^+ by flame photometry. NO_3^--N, F^- and As were measured by the laboratory's standard spectrophotometric and instrumental procedures, and total coliforms and *E. coli* were enumerated as CFU/100 mL. Results were compared with the National Standards for Drinking Water Quality (Pak-EPA, 2008) and the WHO guidelines (WHO, 2022).

Instruments were calibrated before each batch, and blanks, standards and replicate measurements were run throughout. The charge-balance error, CBE = (Σcations − Σanions)/(Σcations + Σanions) × 100 in meq/L, averaged 2.9 ± 2.4% and was within ±5% for 88 samples (94.6%) and within ±10% for 91 (97.8%), so all samples were retained. Two records reporting *E. coli* but no total coliforms were reclassified as coliform-positive, since *E. coli* belongs to the coliform group. One well with an invalid longitude was excluded from mapping and spatial statistics only, and values below detection were set to zero.

3.3 Hydrogeochemical tools

Water types were classified with the Piper (1944) diagram, and the influence of precipitation, rock weathering and evaporation was assessed with Gibbs (1970) diagrams. Salinisation was examined with molar ionic ratios commonly used to identify saline–fresh water interaction (Mondal et al., 2010): Na^+/Cl^-, for which seawater has a value of 0.86, and the Revelle index, RI = $Cl^-/(HCO_3^- +$

CO_3^{2-}) in meq/L (Revelle, 1941). Base exchange was evaluated with the chloro-alkaline indices of Schoeller (1965), CAI-I = $[Cl^- - (Na^+ + K^+)]/Cl^-$ and CAI-II = $[Cl^- - (Na^+ + K^+)]/(SO_4^{2-} + HCO_3^- + CO_3^{2-} + NO_3^-)$, and by plotting $(Na^+ + K^+ - Cl^-)$ against $(Ca^{2+} + Mg^{2+} - HCO_3^- - SO_4^{2-})$, where a slope close to −1 indicates exchange control (Fisher & Mullican, 1997).

Marine influence was quantified with the seawater mixing index of Park et al. (2005), SMI = $0.31(C_{Na}/T_{Na}) + 0.04(C_{Mg}/T_{Mg}) + 0.57(C_{Cl}/T_{Cl}) + 0.06(C_{SO4}/T_{SO4})$, where C is the measured concentration and T a regional background threshold, here the 75th percentile of each ion (Na^+ 352, Mg^{2+} 100, Cl^- 675 and SO_4^{2-} 290 mg/L); SMI > 1 denotes saline influence. The equivalent seawater fraction was estimated from Cl^- as a conservative tracer, $f_{sea} = (Cl_s - Cl_f)/(Cl_sw - Cl_f)$, with Cl_sw = 19,353 mg/L and Cl_f equal to the lowest measured value. Saturation indices of calcite, dolomite, gypsum and halite and the CO_2 partial pressure were calculated at 25 °C using Davies activity coefficients.

3.4 Statistical analysis

Normality was tested with the Shapiro–Wilk test. Because most variables were strongly right-skewed, differences among UCs were tested with the Kruskal–Wallis test and associations with Spearman's ρ. Principal component analysis (PCA) was applied to 13 standardised, log-transformed variables after checking sampling adequacy with the Kaiser–Meyer–Olkin (KMO) measure and Bartlett's test; components with eigenvalues above 1 were retained and varimax-rotated (Kaiser, 1958). Hierarchical cluster analysis (HCA) of standardised, log-transformed major ions used Ward's (1963) linkage on Euclidean distance, the combination shown to give the most interpretable groupings of water-chemistry data (Güler et al., 2002).

3.5 Water quality indices

EWQI was computed for 12 chemical parameters (pH, TDS, HCO_3^-, Cl^-, SO_4^{2-}, Ca^{2+}, Mg^{2+}, Na^+, K^+, NO_3^--N, F^- and TH) following Li et al. (2010) and Amiri et al. (2014). After min–max normalisation of the data matrix (m samples × n parameters), the entropy of parameter j was obtained as $e_j = -(1/\ln m)\, \Sigma\, p_{ij} \ln p_{ij}$, with $p_{ij} = y_{ij}/\Sigma\, y_{ij}$, its weight as $w_j = (1 - e_j)/\Sigma(1 - e_j)$, and the index as EWQI = $\Sigma\, w_j\, q_j$, with $q_j = 100\, C_j/S_j$ and S_j the guideline value. Wells were classed as excellent (<50), good (50–100), medium (100–150), poor (150–200) or extremely poor (>200). For comparison with earlier studies in Sindh, WA-WQI (Brown et al., 1970) was calculated with unit weights $W_n = K/S_n$, $K = 1/\Sigma(1/S_n)$, and quality ratings $Q_n = 100(V_n - V_i)/(S_n - V_i)$, with V_i = 7 for pH and 0 otherwise. WA-WQI was computed with and without turbidity to isolate the effect of this non-chemical variable.

3.6 Health risk assessment

Non-carcinogenic risks from ingestion of NO_3^- (NO_3^--N × 4.427), F^- and As, and the carcinogenic risk from As, were assessed with the USEPA (1989) model: CDI = (C × IR × EF × ED)/(BW × AT), HQ = CDI/RfD, HI = ΣHQ and CR = CDI × CSF. Exposure parameters followed values widely used in groundwater studies (Adimalla & Li, 2019): ingestion rates of 2.5 and 0.78 L/day, body weights of 70 and 15 kg and exposure durations of 30 and 6 years for adults and children, respectively, with an exposure frequency of 365 days/year. The averaging time was ED × 365 days for non-carcinogenic and 70 × 365 days for carcinogenic effects. Reference doses were 1.6 (NO_3^-), 0.06 (F^-) and 0.0003 (As) mg/kg/day, and the As slope factor was 1.5 $(mg/kg/day)^{-1}$. HI > 1 and CR > 10^{-4} were regarded as unacceptable.

Variability and uncertainty were propagated by Monte Carlo simulation with 10,000 iterations per group, an approach increasingly used to complement deterministic estimates (Yadav & Kalkal, 2024; Du et al., 2025; Li et al., 2025). Concentrations were bootstrapped from the measured data, ingestion rate was log-normal (2.5 ± 0.6 L/day for adults; 0.78 ± 0.25 L/day for children) and body weight truncated normal (70 ± 10 kg; 15 ± 3 kg). Sensitivity was expressed as the normalised squared Spearman correlation between each input and HI. Daily Na^+ intake from 2.5 L of drinking water was expressed as a percentage of the WHO adult limit of 2 g/day, because sodium is not covered by the HQ framework.

3.7 Linking microbial and chemical data

Two competing hypotheses were tested. If faecal contamination travels through the aquifer, *E. coli* should co-occur with recharge-borne solutes such as nitrate and chloride and be more frequent in shallow wells (Bagordo et al., 2024). If it enters at the wellhead through broken aprons, unsealed casings or contaminated pump parts, it should co-vary with turbidity and be independent of aquifer chemistry (Ferguson et al., 2011; Knappett et al., 2012). Positive and negative wells were compared with Mann–Whitney U and Fisher's exact tests, and a multivariable logistic regression was fitted with $\log_{10}$ turbidity, depth, NO_3^--N and $\log_{10}$ TDS as predictors. Spatial patterns were examined by plotting each indicator at the GPS location of the corresponding well. Analyses were performed in Python 3.11 (pandas, SciPy, scikit-learn, statsmodels and matplotlib).

3.8 Index agreement and hazard typology

Agreement between EWQI and WA-WQI classes was quantified with the linearly weighted Cohen's kappa (κ_W) and the proportion of identical class assignments, and the influence of each parameter on WA-WQI was evaluated by recomputing the index with one parameter removed at a

time and recording its Spearman correlation with EWQI. To translate the results into management terms, each well was assigned four binary hazard flags: salinity (TDS > 1000 mg/L), fluoride (F^- > 1.5 mg/L or child HQ_F > 1), arsenic (As ≥ 10 µg/L) and faecal contamination (*E. coli* > 0 CFU/100 mL). Independence between the salinity and faecal flags was tested with Fisher's exact test. Wells were then grouped into four intervention classes: safe (no flag); wellhead repair only (faecal flag alone); treatment or source change (one or more geogenic flags without faecal contamination); and combined action (geogenic and faecal flags together).

3.9 Robustness and spatial-scale tests

Three additional tests were used to check the decoupling hypothesis. First, the independence of salinity and *E. coli* was re-tested with Fisher's exact test at TDS thresholds of 500, 1000, 1500, 2000 and 3000 mg/L and for Cl^- > 250 mg/L, SO_4^{2-} > 250 mg/L, F^- > 1.5 mg/L and As ≥ 10 µg/L. Second, the spatial scale of each hazard was assessed with global Moran's I for $\log_{10}$ TDS, $\log_{10}$ Cl^-, F^-, $\log_{10}$ turbidity and *E. coli* presence, using binary distance-band weights of 2, 3 and 5 km between well coordinates (92 wells) and 999 random permutations for significance. If salinity is an aquifer-scale property it should be spatially clustered, whereas wellhead contamination should be spatially random. Third, the performance of turbidity as a field screen for *E. coli* was evaluated by receiver operating characteristic (ROC) analysis, with the area under the curve (AUC) and its 95% confidence interval obtained from 2000 bootstrap resamples, and sensitivity, specificity and predictive values reported for the 5 NTU guideline and the Youden-optimal threshold.

4. Results

4.1 Hydrochemistry and guideline compliance

Descriptive statistics are listed in Table 1. All variables except HCO_3^- departed from normality (Shapiro–Wilk $p < 0.05$), and EC, TDS, Cl^-, Ca^{2+}, Mg^{2+} and TH were strongly right-skewed, so a minority of highly mineralised wells dominates the upper tail. pH (6.80–8.67) was within the 6.5–8.5 range in all but one well. EC ranged from 682 to 11,000 µS/cm (median 1866 µS/cm) and TDS from 409 to 7040 mg/L (median 1120 mg/L). TDS, Cl^- and TH exceeded their guideline values in 58.1%, 54.8% and 53.8% of wells, and Na^+ and SO_4^{2-} in 41.9% and 34.4%. On a milliequivalent basis the cations followed $Na^+ > Mg^{2+} > Ca^{2+} > K^+$ and the anions $Cl^- > HCO_3^- > SO_4^{2-} > NO_3^-$.

Nutrients and trace constituents gave a different picture. NO_3^--N (0.6–9.2 mg/L) was below 10 mg/L in every well, while F^- (0.13–2.80 mg/L) exceeded 1.5 mg/L in six wells (6.5%). Arsenic was detected in ten wells; five contained ≥10 µg/L and the maximum was 25 µg/L, so no well exceeded

the national limit of 50 µg/L. Turbidity varied by more than four orders of magnitude (0.03–980 NTU), and 49.5% of wells exceeded 5 NTU.

Median TDS rose from Gharo (902 mg/L) through Kadi Kazia (1118 mg/L) to Sirani (1332 mg/L), but differences among UCs were not significant for the major ions (Kruskal–Wallis $p = 0.05–0.27$; Fig. 4), showing that variability within each UC exceeds that between them. Only turbidity and F^- ($p < 0.001$, both highest in Sirani) and NO_3^--N ($p = 0.01$) differed significantly.

Table 1. Descriptive statistics of groundwater quality (n = 93), wells exceeding guideline values (Pak-EPA, 2008; WHO, 2022) and medians by union council (GH = Gharo, KK = Kadi Kazia, SR = Sirani) with Kruskal–Wallis p-values.

Parameter	Unit	Min	Max	Mean ± SD	Median	Guideline	n > guideline (%)	Median GH / KK / SR	K–W p
pH	–	6.8	8.67	7.49 ± 0.34	7.5	6.5–8.5	1 (1.1)	7.30 / 7.50 / 7.60	0.097
EC	µS/cm	682	11000	2454 ± 1725	1866	NGVS	–	1504 / 1863 / 2220	0.170
Turbidity	NTU	0.03	980	76.80 ± 178	4.4	5	46 (49.5)	1.75 / 2.14 / 32.48	<0.001
TDS	mg/L	409	7040	1515 ± 1116	1120	1000	54 (58.1)	902 / 1118 / 1332	0.175
Alkalinity	mmol/L	3.4	11	6.38 ± 1.43	6.4	NGVS	–	6.15 / 6.40 / 6.80	0.201
HCO_3^-	mg/L	170	550	320 ± 71.43	320	NGVS	–	315 / 320 / 340	0.275
Cl^-	mg/L	84	2998	477 ± 475	296	250	51 (54.8)	233 / 271 / 376	0.137
SO_4^{2-}	mg/L	18	750	222 ± 143	194	250	32 (34.4)	170 / 182 / 240	0.089
Ca^{2+}	mg/L	36	644	123 ± 89.12	94	NGVS	–	74 / 92 / 112	0.096
Mg^{2+}	mg/L	18	547	86.37 ± 71.11	77	NGVS	–	60 / 61 / 86	0.052
TH (as $CaCO_3$)	mg/L	170	3860	665 ± 510	550	500	50 (53.8)	440 / 530 / 670	0.067
Na^+	mg/L	48	980	254 ± 187	171	200	39 (41.9)	155 / 162 / 229	0.268
K^+	mg/L	4	20	10.95 ± 3.47	11	NGVS	–	10 / 11 / 10	0.260
NO_3^--N	mg/L	0.6	9.2	2.24 ± 1.59	1.77	10	0 (0.0)	1.80 / 1.20 / 1.90	0.009
F^-	mg/L	0.13	2.8	0.75 ± 0.49	0.66	1.5	6 (6.5)	0.43 / 0.66 / 1.05	<0.001
As	µg/L	0	25	0.88 ± 3.35	0	10 (WHO); 50 (NSDWQ)	1 (1.1)	0 / 0 / 0	0.114

NGVS = no guideline value specified; GH = Gharo, KK = Kadi Kazia, SR = Sirani; K–W = Kruskal–Wallis test.

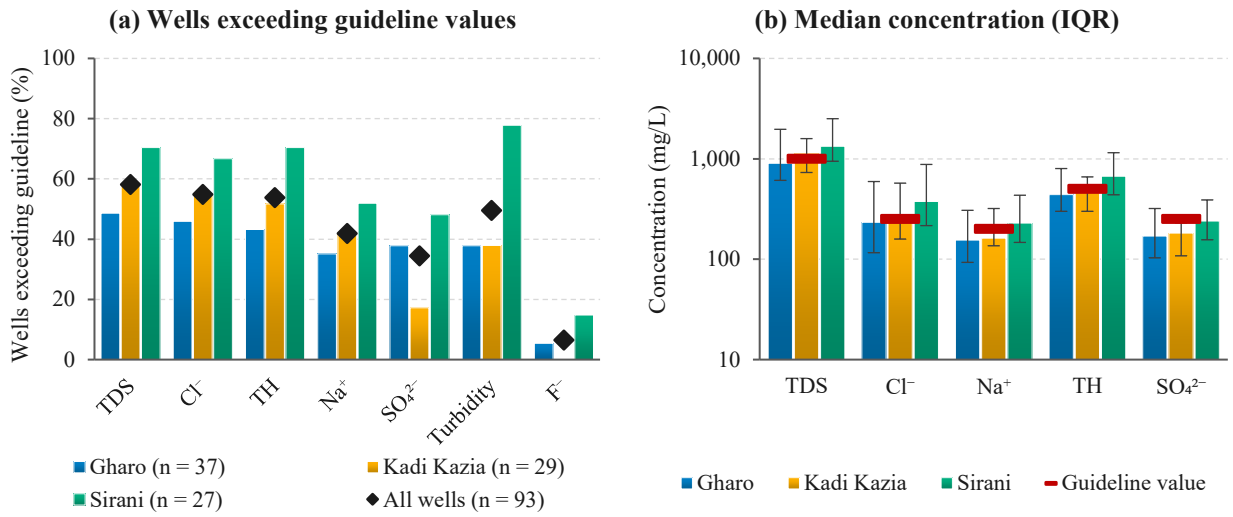


Fig. 4. Guideline compliance and salinity by union council. (a) Percentage of wells exceeding drinking-water guideline values (Pak-EPA, 2008; WHO, 2022); black diamonds show the value for all 93 wells. (b) Median concentrations with interquartile range (error bars) on a logarithmic scale; red bars mark the guideline value for each parameter.

4.2 Water types and controlling processes

Sixty-one samples (65.6%) plotted in the mixed Ca–Mg–Cl–SO_4 field of the Piper diagram and 29 (31.2%) in the Na–Cl–SO_4 field, while only three were of bicarbonate type (Fig. 5). The Ca–HCO_3 signature typical of recently recharged water has therefore been almost entirely overprinted. In the Gibbs diagrams (Fig. 6), $Na^+/(Na^+ + Ca^{2+})$ ranged from 0.38 to 0.82 and $Cl^-/(Cl^- + HCO_3^-)$ from 0.32 to 0.92, and samples extended from the rock-dominance field towards the evaporation–crystallisation field as TDS increased. Water–rock interaction has thus been progressively overprinted by evaporative concentration.

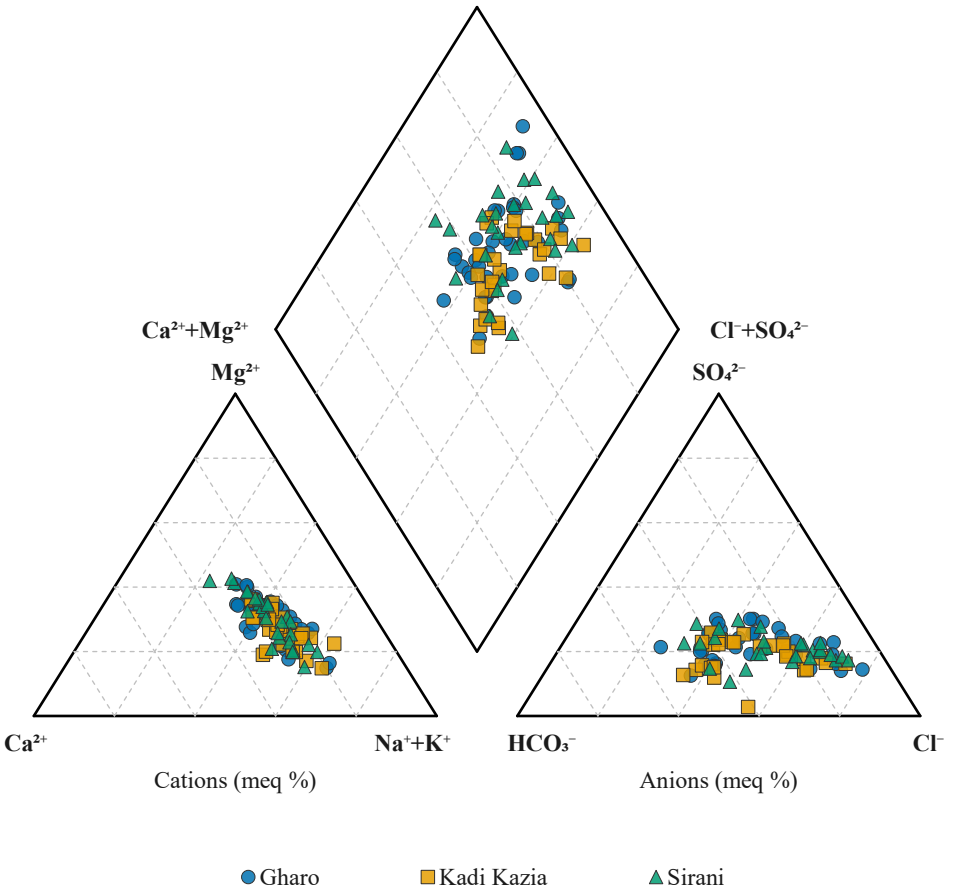


Fig. 5. Piper diagram of groundwater samples by union council. Cation (left) and anion (right) triangles are in meq %; the central diamond shows the combined water type.

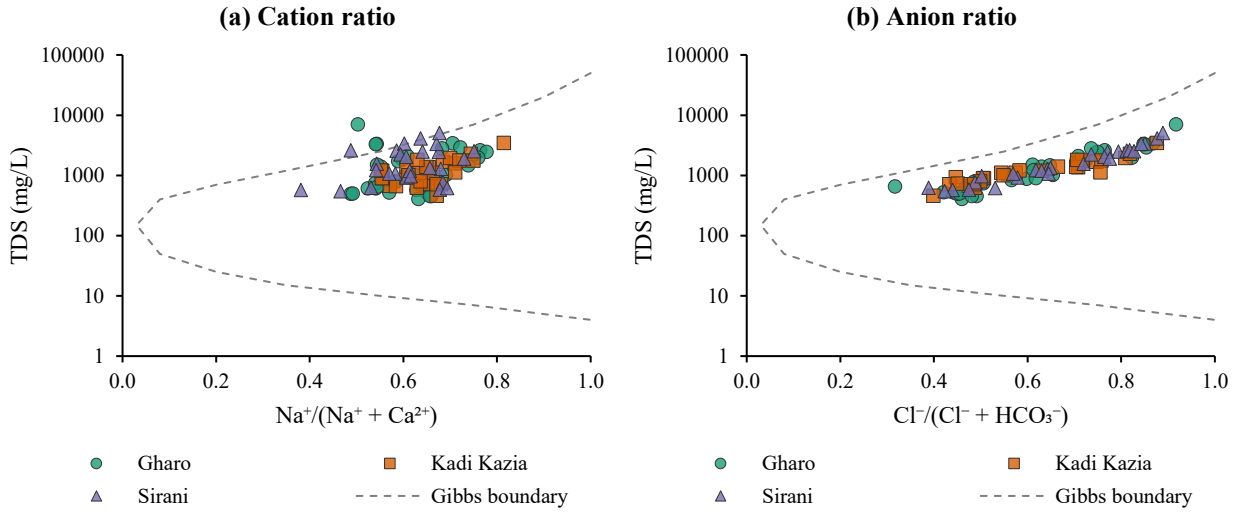


Fig. 6. Gibbs diagrams of (a) $Na^+/(Na^+ + Ca^{2+})$ and (b) $Cl^-/(Cl^- + HCO_3^-)$ against TDS, by union council. The dashed line shows the approximate Gibbs boundary.

Ionic ratios separate this overprint into distinct processes (Table 2; Fig. 7). The molar Na^+/Cl^- ratio averaged 1.00 but fell below the seawater value of 0.86 in 31 wells (33.3%), and CAI-I was positive

in 44 wells (47.3%). Together these indicate reverse ion exchange, in which Na^+ supplied by saline water is adsorbed on clays and Ca^{2+} and Mg^{2+} are released. Wells with $Na^+/Cl^- > 1$ and negative CAI instead reflect direct exchange or silicate weathering. Across all samples the exchange plot gave a slope of −0.95 ($R^2 = 0.97$; Fig. 7b), demonstrating that base exchange in the clay-rich deltaic sediments controls composition over the whole salinity range.

The Revelle index classed 37 wells as slightly, 30 as moderately and 25 as strongly affected by saline water. SMI exceeded 1 in 22 wells (23.7%), and the Cl^--based seawater fraction averaged 2.0% with a maximum of 15.1%. Most samples were supersaturated with calcite (86.0%) and dolomite (92.5%) but undersaturated with gypsum and halite (Fig. 7d), and log pCO_2 (−3.17 to −1.27) was one to two orders of magnitude above atmospheric. Carbonate saturation therefore caps Ca^{2+} and HCO_3^-, while Na^+, Cl^- and SO_4^{2-} remain free to accumulate.

Table 2. Hydrochemical ratios, indices and saturation indices used to identify salinisation processes.

Index	Result (n = 93)	Interpretation
Hydrochemical facies (Piper)	Ca–Mg–Cl–SO_4 61 (65.6%); Na–Cl–SO_4 29 (31.2%); Na–HCO_3 2; Ca–Mg–HCO_3 1	Mixed Ca–Mg–Cl evolving to Na–Cl
Na^+/Cl^- (molar)	0.38–1.61 (mean 1.00); <0.86 in 31 (33.3%)	Reverse exchange in one-third; Na excess elsewhere
Revelle index (Cl^-/HCO_3^-)	<0.5: 1; 0.5–1.3: 37; 1.3–2.8: 30; >2.8: 25	Slight to strong saline influence in 59%
CAI-I / CAI-II	CAI-I > 0 in 44 (47.3%); range −0.70 to 0.61	Both direct and reverse ion exchange
(Ca+Mg)−(HCO_3+SO_4) vs (Na+K)−Cl	slope −0.95, $R^2 = 0.97$	Cation exchange is a first-order control
Seawater mixing index (SMI)	0.15–3.56; SMI > 1 in 22 (23.7%)	Saline influence in about one-quarter of wells
Seawater fraction (Cl^-)	mean 2.0%, max 15.1%	≤15% seawater-equivalent salinity
SI calcite / dolomite	0.42 / 1.00 (supersaturated in 80 / 86)	Carbonate saturation
SI gypsum / halite	−1.29 / −5.81 (all < 0)	Evaporite dissolution not limited by saturation
log pCO_2 (atm)	−3.17 to −1.27 (mean −2.03)	Soil-CO_2-charged recharge

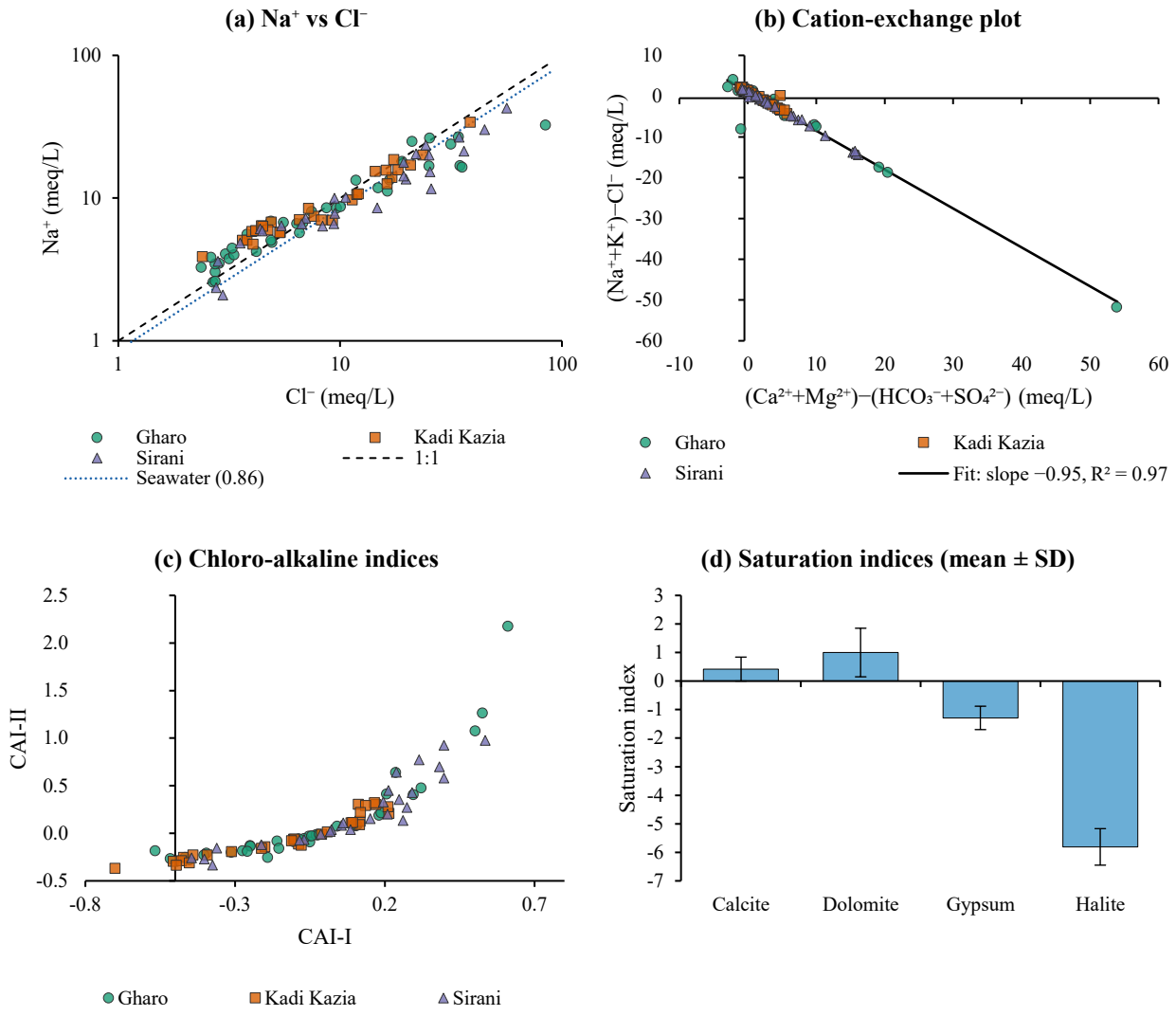


Fig. 7. Process diagnostics: (a) Na^+ vs Cl^- (meq/L, log scale) with 1:1 and seawater (0.86) lines; (b) cation-exchange plot with fitted regression; (c) chloro-alkaline indices CAI-I vs CAI-II (positive values indicate reverse ion exchange); (d) mean (± SD) saturation indices of calcite, dolomite, gypsum and halite.

4.3 Multivariate structure

EC, TDS, Cl^-, Na^+, Ca^{2+}, Mg^{2+} and SO_4^{2-} were strongly inter-correlated (Spearman $\rho > 0.8$; Fig. 8a), and NO_3^--N correlated with both Cl^- and TDS ($\rho = 0.69$). The data were well suited to factor analysis (KMO = 0.893; Bartlett's $\chi^2 = 2178.5$, $p < 0.001$). Two varimax factors explained 77.1% of the variance (Table 3; Fig. 8b). VF1 (65.9%) loaded strongly on EC, TDS and Cl^- (0.99), Ca^{2+}, Na^+, Mg^{2+}, SO_4^{2-}, K^+, HCO_3^- and NO_3^--N (0.78–0.97) and represents an integrated salinisation factor. VF2 (11.2%) loaded on pH (0.72), F^- (0.71) and turbidity (0.60), grouping fluoride with alkaline conditions. Because nitrate loaded with the salts rather than on a separate factor, it appears to be concentrated together with them by evaporation and irrigation return flow.

Table 3. Varimax-rotated factor loadings.

Variable	VF1	VF2
pH	−0.18	0.72
EC	0.99	0.07
TDS	0.99	0.07
HCO_3^-	0.81	0.10
Cl^-	0.99	0.05
SO_4^{2-}	0.89	0.13
Ca^{2+}	0.97	0.10
Mg^{2+}	0.93	0.09
Na^+	0.94	0.02
K^+	0.83	−0.07
NO_3^--N	0.78	−0.05
F^-	0.32	0.71
Turbidity	0.18	0.60
Eigenvalue (unrotated)	8.64	1.38
Variance explained (%)	65.9	11.2

Loadings > 0.60 indicate a strong contribution to the factor.

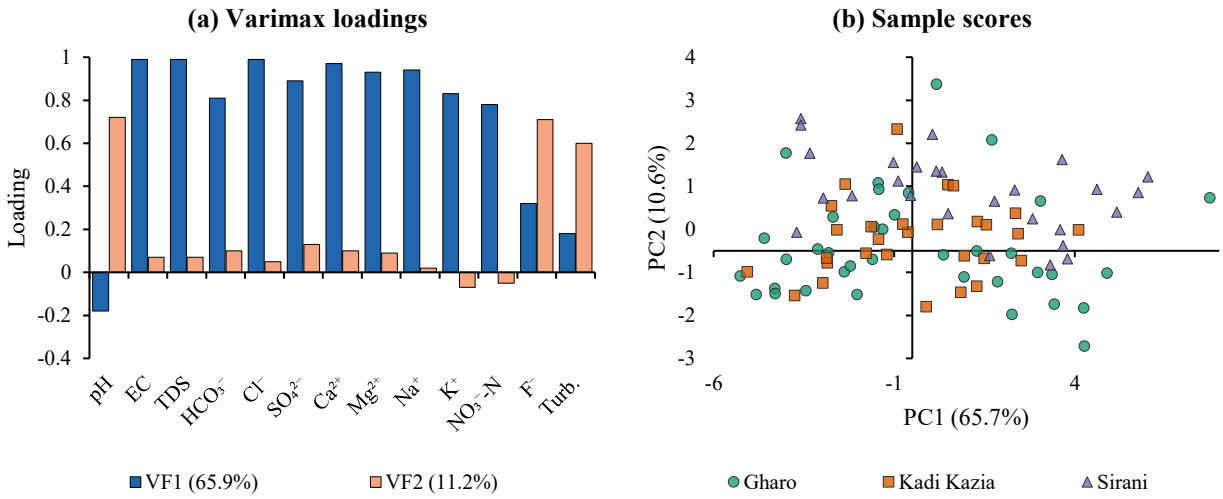


Fig. 8. (a) Varimax-rotated loadings of the two retained factors; (b) principal-component scores of the 93 wells by union council.

HCA resolved three groups (Fig. 9). Cluster C1 (n = 49; median TDS 731 mg/L, Cl^- 157 mg/L) is fresh to slightly mineralised water. Cluster C2 (n = 29; TDS 1722 mg/L, Cl^- 579 mg/L) is brackish water bearing ion-exchange signatures. Cluster C3 (n = 15; TDS 3334 mg/L, Cl^- 1220 mg/L, median SMI 1.6, NO_3^--N 4.3 mg/L) is saline water with the strongest marine and evaporative imprint; nine of its 15 wells were in Sirani.

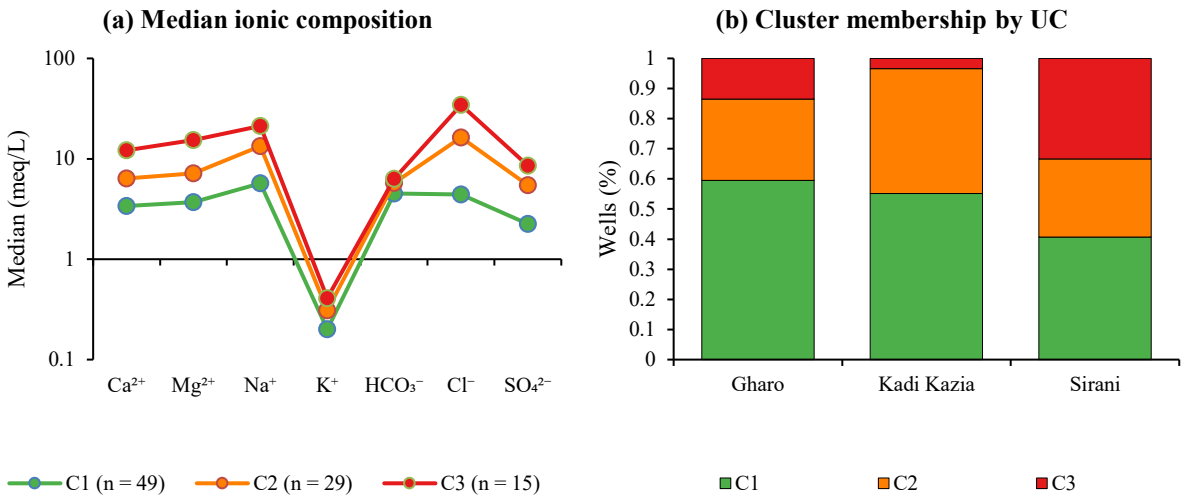


Fig. 9. Hierarchical cluster analysis: (a) median ionic composition (meq/L, log scale) of clusters C1 (fresh), C2 (brackish) and C3 (saline); (b) share of each cluster in each union council.

4.4 Water quality indices

The entropy method gave the largest weights to Cl^- (0.151), TDS (0.110), NO_3^--N (0.104) and Ca^{2+}, Mg^{2+} and TH (about 0.10 each), and the smallest to pH, HCO_3^- and K^+ (about 0.03) (Table 4a). EWQI ranged from 35.7 to 620.8 (median 101.7): 10 wells (10.8%) were excellent, 36 (38.7%) good, 19 (20.4%) medium, 15 (16.1%) poor and 13 (14.0%) extremely poor (Table 4b), so half of the wells (50.5%) scored above 100. Sirani had no excellent well and the most extremely poor wells (7 of 27).

WA-WQI distributed weight in a completely different way. Because W_n is inversely proportional to the guideline value, F^- (1.5 mg/L) received 50.6% of the total weight and turbidity (5 NTU) 15.2%, followed by As, NO_3^--N and K^+ (6–8% each). TDS, Cl^- and Na^+, the variables that define the water-quality problem in this aquifer, together received less than 1%. WA-WQI values (15.96–3042) were therefore almost perfectly rank-correlated with turbidity ($\rho = 0.89$) but only weakly with EWQI ($\rho = 0.36$; Fig. 10b). Of the 32 wells rated unsuitable, most were turbid rather than saline: excluding turbidity lowered the maximum WA-WQI from 3042 to 192, reduced the number of unsuitable wells from 32 to 3 and raised the correlation with EWQI to $\rho = 0.61$ (Fig. 10c). Agreement between the two indices was poor (weighted $\kappa = 0.20$; identical classes in 30.1% of wells), and only 3 of the 15 worst-ranked wells were common to both. Thirteen of the 32 wells rated unsuitable by WA-WQI were excellent or good under EWQI, whereas 7 wells rated poor or extremely poor by EWQI appeared excellent or good under WA-WQI. Dropping one parameter at a time showed that turbidity alone controlled this disagreement: its removal raised the correlation with EWQI from 0.36 to 0.61, whereas removing any other parameter changed it by less than 0.03 (Fig. 10d).

Table 4a. Entropy and weights of EWQI parameters compared with WA-WQI unit weights.

Parameter	Standard S_j	Entropy e_j	EWQI weight w_j	WA-WQI weight W_n*
pH	8.5	0.972	0.033	0.0893
TDS	1000	0.908	0.110	0.0008
HCO_3^-	500	0.972	0.033	–
Cl^-	250	0.873	0.151	0.0030
SO_4^{2-}	250	0.948	0.061	0.0030
Ca^{2+}	75	0.914	0.102	0.0101
Mg^{2+}	50	0.914	0.102	0.0152
Na^+	200	0.920	0.095	0.0038
K^+	12	0.971	0.034	0.0632
NO_3^--N	10	0.912	0.104	0.0759
F^-	1.5	0.938	0.074	0.5060
TH	500	0.914	0.101	0.0015

* WA-WQI weights also include EC (0.0005), turbidity (0.152) and As (0.076).

Table 4b. Distribution of wells among water-quality classes under EWQI and WA-WQI (with and without turbidity).

Class (EWQI range)	EWQI n (%)	Class (WA-WQI range)	WA-WQI all n (%)	WA-WQI no turbidity n (%)
Excellent (<50)	10 (10.8)	Excellent (0–25)	13 (14.0)	12 (12.9)
Good (50–100)	36 (38.7)	Good (26–50)	23 (24.7)	41 (44.1)
Medium (100–150)	19 (20.4)	Poor (51–75)	18 (19.4)	28 (30.1)
Poor (150–200)	15 (16.1)	Very poor (76–100)	7 (7.5)	9 (9.7)
Extremely poor (>200)	13 (14.0)	Unsuitable (>100)	32 (34.4)	3 (3.2)

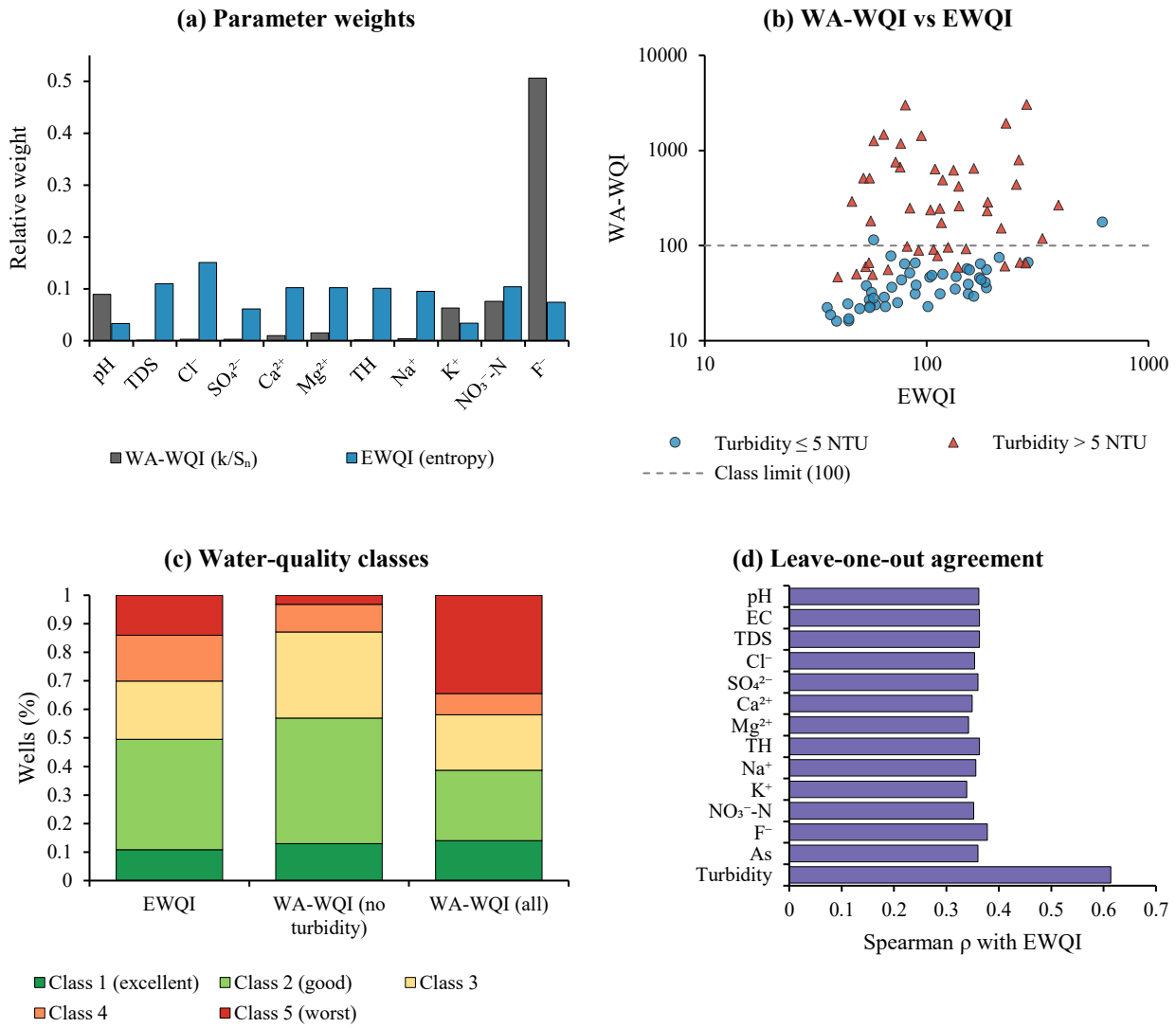


Fig. 10. Water quality index comparison: (a) parameter weights under WA-WQI and EWQI; (b) WA-WQI vs EWQI by turbidity class (log–log); (c) class distributions under EWQI and WA-WQI with and without turbidity; (d) Spearman correlation of WA-WQI with EWQI after removing each parameter in turn (full index $\rho = 0.36$).

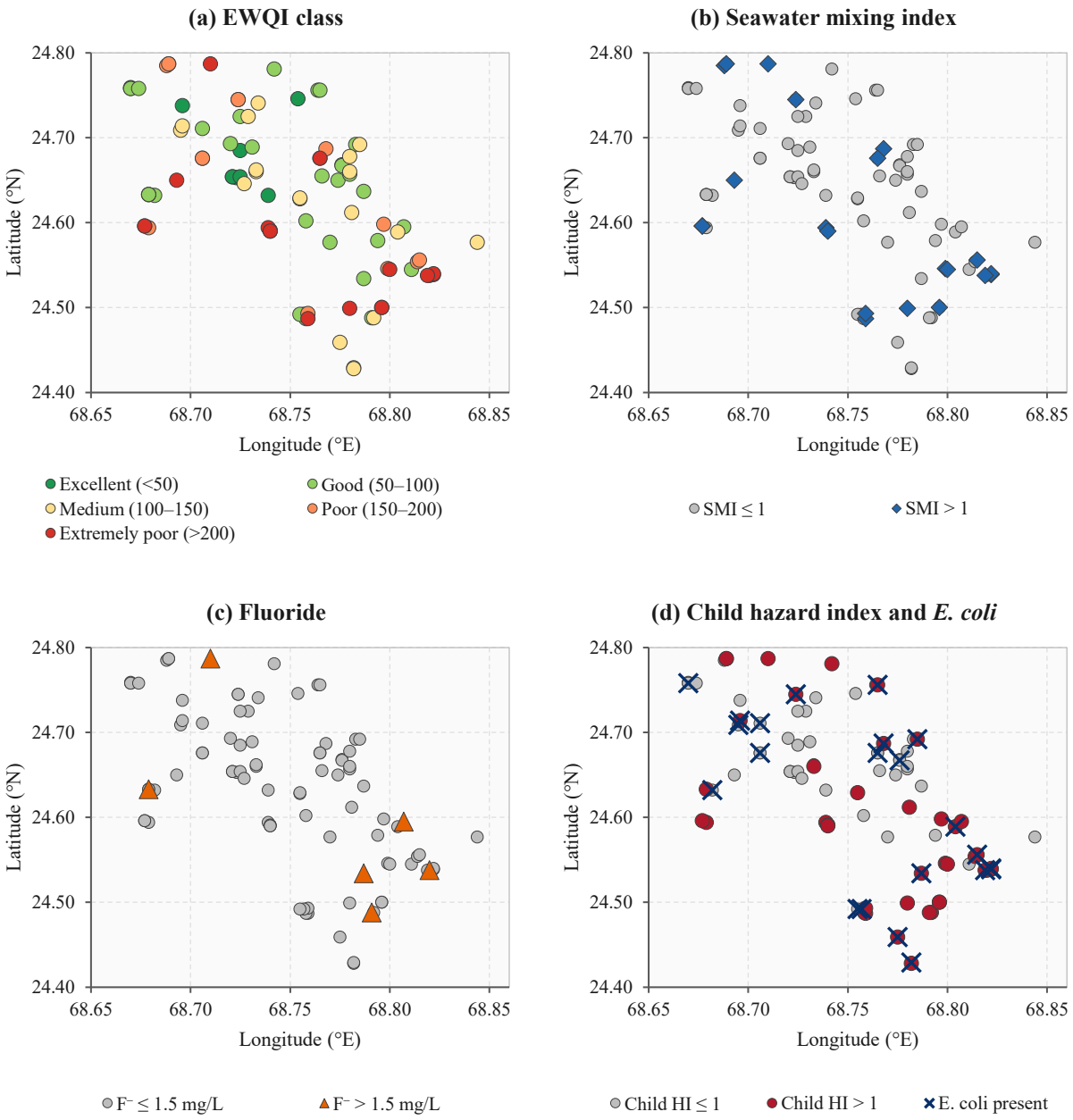


Fig. 11. Spatial distribution of water-quality and risk indicators at the sampled wells: (a) EWQI class; (b) seawater mixing index; (c) fluoride relative to the 1.5 mg/L guideline; (d) child hazard index, with *E. coli*-positive wells marked (×).

4.5 Microbial quality and its relation to chemistry

Total coliforms were present in 27 wells (29.0%) and *E. coli* in 22 (23.7%), at 1–80 CFU/100 mL (median 3.5); all positive wells failed the zero-tolerance criterion. Positive wells occurred in every UC (Gharo 8, Kadi Kazia 4, Sirani 10; χ^2 $p = 0.12$) and in every hydrochemical cluster, with no concentration in the saline zone (Fig. 11d). They were, however, much more turbid than negative wells (median 145.5 vs 2.2 NTU; $p < 0.001$; Fig. 12a): 18 of the 22 positive wells exceeded 5 NTU, against 28 of the 71 negative wells (Fisher's exact test, OR = 6.91, $p < 0.001$).

Positive and negative wells did not differ in depth ($p = 0.79$), NO_3^--N ($p = 0.45$), TDS ($p = 0.91$) or Cl^- ($p = 0.96$) (Table 5). In the multivariable logistic model, turbidity was the only significant predictor (OR = 4.18 per $\log_{10}$ NTU; 95% CI 2.20–7.97; $p < 0.001$), whereas the confidence intervals for depth, nitrate and TDS all included unity (Fig. 12b).

Table 5. Comparison of *E. coli*-positive and -negative wells and multivariable logistic regression results.

Variable	***E. coli* present (n = 22)**	***E. coli* absent (n = 71)**	**Statistic**
Turbidity (NTU), median	145.5	2.2	$p < 0.001$ (M–W)
Turbidity > 5 NTU, n	18 of 22	28 of 71	OR 6.91; $p < 0.001$ (Fisher)
Well depth (m), median	22.5	24.0	$p = 0.79$ (M–W)
NO_3^--N (mg/L), median	1.9	1.6	$p = 0.45$ (M–W)
TDS (mg/L), median	1152	1120	$p = 0.91$ (M–W)
Cl^- (mg/L), median	315	292	$p = 0.96$ (M–W)
Logit: $\log_{10}$ turbidity	—	—	OR 4.18 (2.20–7.97); $p < 0.001$
Logit: depth (per m)	—	—	OR 0.95 (0.85–1.05); $p = 0.32$
Logit: NO_3^--N (per mg/L)	—	—	OR 0.91 (0.52–1.59); $p = 0.74$
Logit: $\log_{10}$ TDS	—	—	OR 0.58 (0.03–13.4); $p = 0.73$

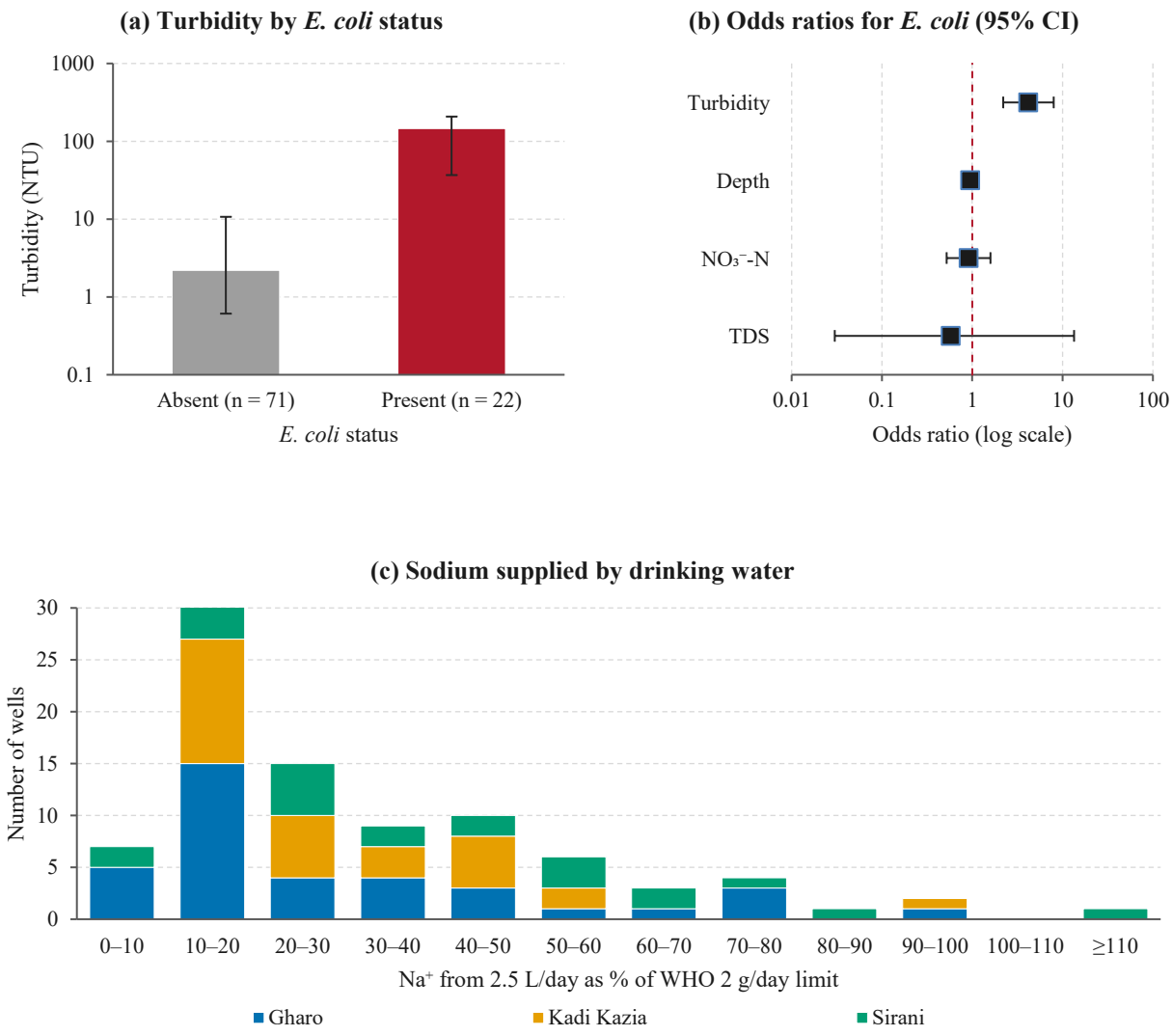


Fig. 12. Microbial and sodium results: (a) median turbidity (error bars = interquartile range) in *E. coli*-negative and -positive wells; (b) odds ratios (95% CI) from the multivariable logistic model (turbidity and TDS entered as $\log_{10}$ values), with the dashed line at OR = 1; (c) sodium supplied by 2.5 L/day of drinking water as a share of the WHO 2 g/day limit, by union council.

4.6 Human health risk

In the deterministic assessment, HI exceeded 1 in 20 wells (21.5%) for adults and 39 wells (41.9%) for children; the mean child HI was 1.13 and the maximum 7.85 (Table 6). F^- was the main contributor, with HQ > 1 in 4 wells for adults and 15 for children. As produced HQ > 1 in the five wells with As ≥ 10 µg/L, whereas NO_3^- exceeded HQ = 1 only for children and only in two wells. The carcinogenic risk from As exceeded 10^{-4} for adults in eight wells (maximum 5.7×10^{-4}) and exceeded 10^{-6} in all ten wells with detectable As.

Monte Carlo simulation gave median (95th percentile) HI values of 0.63 (1.91) for adults and 0.94 (3.06) for children, and probabilities of HI > 1 of 23.6% and 46.1% (Fig. 13a). F^- concentration accounted for 43–49% of the output variance, followed by NO_3^- concentration (19–21%), As

concentration (13–15%) and ingestion rate (11–18%); body weight had a small negative effect (Fig. 13c). Drinking water alone supplied on average 31.7% of the WHO daily sodium limit, more than half of it in 17 wells and up to 122.5% in the most saline well (Fig. 12c).

Table 6. Deterministic and probabilistic (Monte Carlo, 10,000 iterations) health-risk indices for adults and children.

Group	Index	Deterministic range (mean)	n > 1	MC P50 / P95	MC P(>1) %
Adults	HQ NO_3^-	0.059–0.91 (0.22)	0	0.170 / 0.593	0.5
Adults	HQ F^-	0.077–1.67 (0.45)	4	0.387 / 1.120	7.0
Adults	HQ As	0.000–2.98 (0.10)	5	0.000 / 0.920	4.5
Adults	HI	0.156–5.39 (0.77)	20	0.634 / 1.913	23.6
Adults	CR (As)	0–5.74 × 10^{-4}	8 (>10^{-4})	–	–
Children	HQ NO_3^-	0.086–1.32 (0.32)	2	0.255 / 0.968	4.5
Children	HQ F^-	0.113–2.43 (0.65)	15	0.565 / 1.789	22.0
Children	HQ As	0.000–4.33 (0.15)	5	0.000 / 1.258	6.1
Children	HI	0.228–7.85 (1.13)	39	0.935 / 3.057	46.1
Children	CR (As)	0–1.67 × 10^{-4}	1 (>10^{-4})	–	–

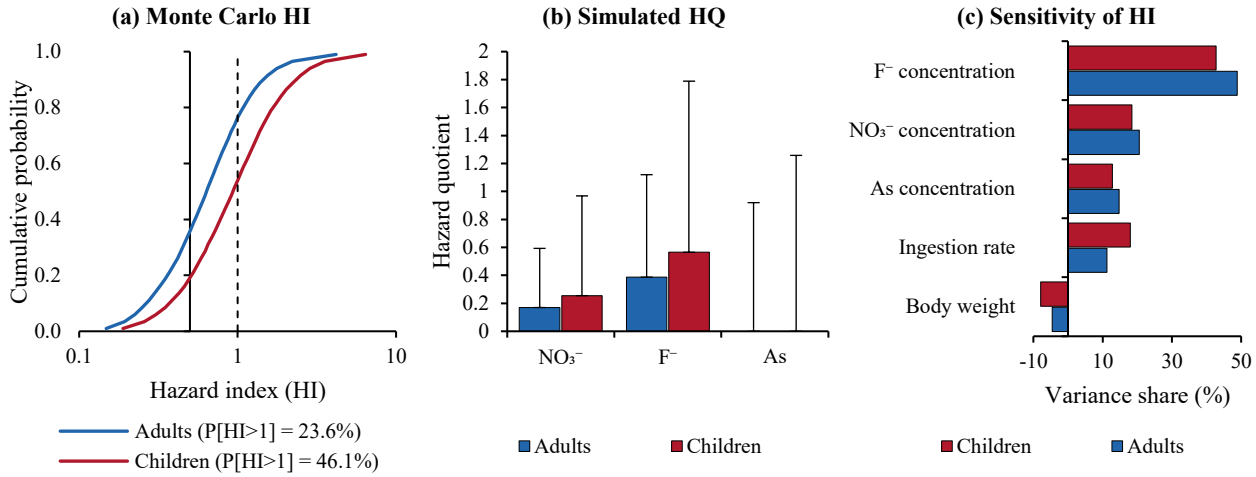


Fig. 13. Health risk: (a) cumulative distributions of Monte Carlo HI for adults and children; (b) simulated HQ by constituent (bars = median, whiskers = 95th percentile); (c) contribution of input variables to HI variance.

4.7 Co-occurrence of hazards and intervention classes

Combining the four hazard flags showed that only 25 wells (26.9%) were free of salinity, fluoride, arsenic and faecal contamination (Fig. 14a). Forty-four wells (47.3%) carried one hazard, 20 (21.5%) two and 4 (4.3%) three; salinity alone was the most frequent profile (33 wells), followed by salinity with faecal contamination (10) and faecal contamination alone (8). The salinity and faecal flags were statistically independent: *E. coli* occurred in 22.2% of saline wells and 25.6% of non-

saline wells (Fisher's exact test, OR = 0.83, p = 0.81). The co-occurrence that does exist is therefore what would be expected by chance from two unrelated processes.

Translated into intervention classes (Table 7; Fig. 14b), 46 wells (49.5%) required treatment or a new source for geogenic hazards alone, 8 (8.6%) could be made safe by wellhead repair alone, and 14 (15.1%) needed both. The classes were unevenly distributed: safe wells made up 32.4% of Gharo and 37.9% of Kadi Kazia but only 7.4% of Sirani, where 29.6% of wells required combined action.

Table 7. Intervention classes derived from the hazard typology, with the number (%) of wells in each union council.

Intervention class	Hazard flags	All wells n (%)	Gharo n (%)	Kadi Kazia n (%)	Sirani n (%)
Safe	None	25 (26.9)	12 (32.4)	11 (37.9)	2 (7.4)
Wellhead repair only	Faecal only	8 (8.6)	5 (13.5)	1 (3.4)	2 (7.4)
Treatment or source change	Salinity, F^- and/or As; no faecal	46 (49.5)	17 (45.9)	14 (48.3)	15 (55.6)
Combined action	Geogenic + faecal	14 (15.1)	3 (8.1)	3 (10.3)	8 (29.6)
Total		93 (100)	37 (100)	29 (100)	27 (100)

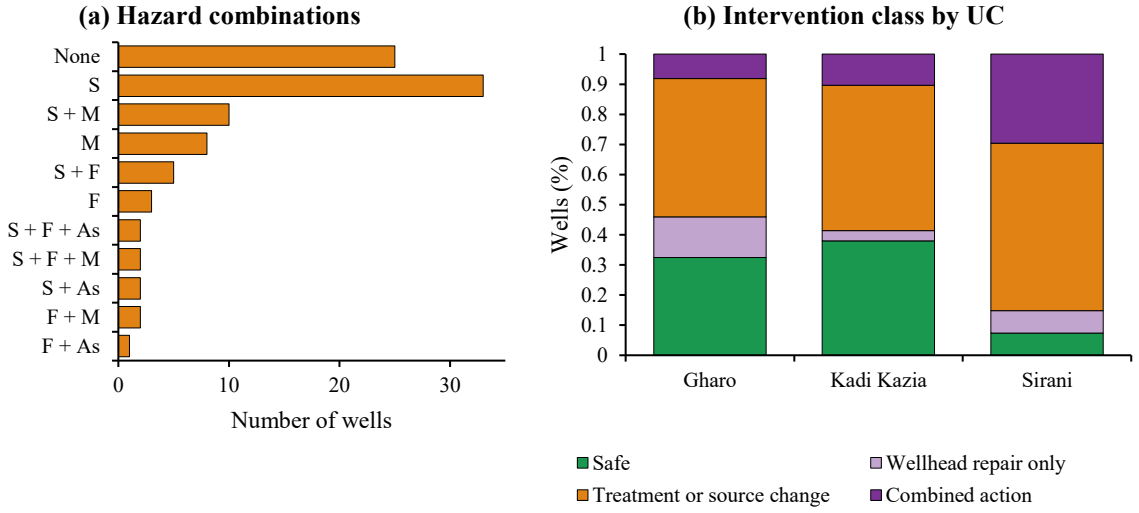


Fig. 14. (a) Number of wells by hazard combination (S = salinity, TDS > 1000 mg/L; F = fluoride, F^- > 1.5 mg/L or child HQ > 1; As = arsenic ≥ 10 µg/L; M = *E. coli* present); (b) intervention classes by union council.

4.8 Robustness of the decoupling and spatial scale of the hazards

The independence of the geogenic and faecal hazards did not depend on the threshold chosen. Odds ratios for *E. coli* in saline versus non-saline wells were 0.83 (TDS > 1000 mg/L; p = 0.81), 0.99 (>

1500 mg/L; p = 1.00), 0.93 (> 2000 mg/L; p = 1.00) and 0.91 (> 3000 mg/L; p = 1.00); at > 500 mg/L only five wells were non-saline and none contained *E. coli* (p = 0.34), and none of the chemical flags tested (Cl^-, SO_4^{2-}, F^-, As) was significantly associated with *E. coli* (all $p \geq 0.33$). The number of *E. coli* colonies was likewise unrelated to TDS (Spearman $\rho = 0.02$, p = 0.87).

The two hazards also operated at different spatial scales. Salinity was significantly clustered at every distance band ($\log_{10}$ TDS: Moran's I = 0.36 at 2 km, p = 0.002; 0.26 at 3 km, p = 0.002; 0.10 at 5 km, p = 0.03), as were Cl^- and F^- ($p \leq 0.04$). In contrast, *E. coli* presence showed no significant spatial autocorrelation at any band (I = 0.21, p = 0.052 at 2 km; 0.12, p = 0.13 at 3 km; 0.06, p = 0.11 at 5 km). Turbidity was spatially clustered (I = 0.46 at 2 km, p = 0.001), suggesting that pump construction and maintenance practices are shared within villages.

Turbidity discriminated well between *E. coli*-positive and -negative wells (AUC = 0.82; 95% CI 0.71–0.93). At the 5 NTU guideline, sensitivity was 81.8%, specificity 60.6%, positive predictive value 39.1% and negative predictive value 91.5%; the Youden-optimal threshold of about 15 NTU retained the same sensitivity (81.8%) while raising specificity to 78.9%. A clear well (≤ 5 NTU) was therefore very unlikely to contain *E. coli*.

5. Discussion

5.1 Two hazards, two scales: a decoupling framework for coastal drinking water

The central result of this study is that drinking-water risk in the Badin aquifer is not one problem but two, with different origins, spatial scales and remedies. The geogenic hazard is an aquifer property: it is captured by a single salinity factor, structured into hydrochemical clusters and governed by evaporation, cation exchange and marine mixing that operate over kilometres. The faecal hazard is a wellhead property: it is independent of salinity (OR = 0.83, p = 0.81), shows no relation to nitrate or depth and is predicted only by turbidity, which reflects the integrity of the individual pump. The spatial statistics make the difference in scale explicit: salinity and fluoride are significantly clustered over 2–5 km, whereas *E. coli* shows no significant spatial autocorrelation at any distance band (Section 4.8), and the independence of the two hazards holds at every salinity threshold tested. Because the two hazards are statistically independent, their overlap in 15% of wells arises from chance co-location rather than a shared pathway, and neither can be inferred from the other.

This decoupling has direct consequences for assessment practice. An aggregated 'unsafe' label, or a single index value, merges hazards that require a reverse-osmosis plant with hazards that require a

cement apron, and so cannot rank interventions. The hazard typology developed here resolves this: one-quarter of wells are already safe, one in twelve needs only wellhead repair, and about half need treatment or a new source irrespective of sanitation. The framework is transferable to other deltaic aquifers where salinisation and poor sanitation coexist, such as the Ganges–Brahmaputra and Mekong deltas (Syvitski et al., 2009), and requires only data that routine monitoring programmes already collect. Sections 5.2–5.5 examine each component of the framework in turn.

5.2 A layered model of salinisation

The diagnostics point to several processes acting in sequence on the same groundwater. Recharge from canal seepage and the monsoon carries soil CO_2, dissolves carbonates and initially acquires Ca–Mg–HCO_3 character, but it reaches calcite and dolomite saturation quickly (cluster C1). Where the water table is shallow and evaporative demand high, conservative solutes are then concentrated, as shown by the Gibbs trend and by the co-loading of NO_3^- and Cl^- on VF1. Exchange with deltaic clays redistributes cations at every stage (exchange slope −0.95), yielding Ca–Mg–Cl water where Na^+ is adsorbed and Na–Cl water where it is released (C2). On top of this, about a quarter of the wells, mostly in Sirani, carry an additional saline component identified by SMI > 1 (C3).

The 31 wells that combine $Na^+/Cl^- < 0.86$ with positive CAI provide the clearest evidence of active intrusion, because reverse exchange operates only where Na-rich water displaces fresher pore water (Mondal et al., 2010). The same pairing of reverse ion exchange and seawater mixing controls groundwater evolution in other South Asian coastal aquifers (Agarwal & Dhakate, 2024; Goswami & Rai, 2025), where fine sand and silt layers favour saline seepage (Sarkar et al., 2026). The low seawater fractions estimated here (mean 2%, maximum 15%) matter for interpretation: the aquifer is degraded not by wholesale replacement of fresh water but by small saline admixtures into thin freshwater bodies, which are enough to push TDS beyond potable limits and are sensitive to pumping and screen depth (Werner et al., 2013). The saline end-member may be modern seawater, relict marine pore water in deltaic clays or saline drainage effluent, and major ions alone cannot fully separate these sources.

These findings agree with earlier reports of salinity-driven unsuitability in coastal Sindh (Alamgir et al., 2016) and in the Indus Delta and Sujawal (Solangi et al., 2019a, 2020), but go further by apportioning the processes and showing that evaporation and base exchange act throughout the aquifer whereas marine mixing is spatially restricted. The distinction matters because continued erosion and saline encroachment of the delta front (Giosan et al., 2006; Aeman et al., 2023),

together with projected climate-driven saltwater intrusion (Mueller et al., 2024), are likely to enlarge the marine-affected zone.

5.3 Index choice changes the management picture

WA-WQI is the most widely used index in Pakistani and South Asian groundwater studies, but its weights encode the numerical size of each guideline value rather than the hazard or variability of a parameter (Brown et al., 1970). In a saline aquifer this produces a misleading result: nearly all weight falls on parameters with small standards (F^-, turbidity and As), and almost none on the salinity variables that actually make the water undrinkable. The index then behaves as a turbidity–fluoride index, and its extreme values, here above 3000, are produced by a few turbid wells whose turbidity reflects pump condition rather than aquifer quality. This is a concrete example of the weighting and eclipsing problems highlighted in reviews of index models (Uddin et al., 2021). The weighted κ of 0.20 and the reclassification of 13 'unsuitable' wells as chemically good quantify how far this bias distorts the ranking of sources, and the leave-one-out test (Fig. 10d) traces it almost entirely to a single non-chemical variable.

Entropy weighting avoids this structural bias by allocating weight according to how much each parameter varies among wells (Li et al., 2010; Amiri et al., 2014). In Badin it ranked Cl^- and TDS highest, in line with the PCA, and its spatial pattern matched the hydrochemical clusters. Future assessments should therefore report EWQI or another data-driven index alongside WA-WQI, exclude non-conservative physical variables such as turbidity from chemical-suitability indices, and publish the parameter weights so that results can be compared between studies.

5.4 Faecal contamination is a wellhead problem

The microbial results discriminate clearly between the hypotheses set out in Section 3.7. Contamination transported through the aquifer should accompany nitrate and chloride and be more frequent in shallow wells (Bagordo et al., 2024), yet positive wells had the same depth, nitrate and salinity as negative ones, and *E. coli* occurred in fresh and saline clusters alike. The only strong predictor was turbidity, which in a fine-grained aquifer signals the entry of surface water and particles through cracked aprons, unsealed casings, priming with surface water or ponding around the pump. This pattern matches evidence from Bangladesh that faecal contamination follows unsealed well annuli (Knappett et al., 2012) and the pumps themselves (Ferguson et al., 2011) rather than aquifer chemistry (van Geen et al., 2011).

The microbial hazard can therefore be tackled pump by pump at low cost, through apron and seal repair, drainage of the pump surroundings, avoidance of priming with untreated water and

household disinfection. Because sanitary-inspection scores predict *E. coli* poorly (Ercumen et al., 2017; Natishah et al., 2025), the strong link with turbidity has practical value: turbidity discriminated contaminated from clean wells with an AUC of 0.82, and a well reading ≤ 5 NTU had a 91.5% probability of being free of *E. coli*. A simple field turbidity reading could therefore be used to target bacteriological testing. Faecal contamination generally increases in the wet season (Kostyla et al., 2015), so the prevalence reported here from a single campaign is probably a lower bound.

5.5 Health implications and intervention priorities

Fluoride, not nitrate, dominates the non-carcinogenic risk, and children face roughly twice the adult probability of HI > 1. The risk is concentrated in Sirani, where F^- co-varies with pH (VF2), consistent with the alkaline, Ca-poor conditions that favour fluoride enrichment in the Badin aquifer (Talpur et al., 2020), elsewhere in Sindh (Ullah et al., 2025), including the Dadu canal command area (Ullah et al., 2026). Probabilistic risks of similar magnitude, again highest for children, have been reported for fluoride, nitrate and arsenic in other South Asian and semi-arid aquifers (Raicy et al., 2026; Yadav & Kalkal, 2024; Du et al., 2025). Nitrate, although co-concentrated with the salts, stayed below the guideline in every well and contributed little to HI, in contrast to many agricultural aquifers where it is the leading concern (Ward et al., 2018).

Arsenic is infrequent but consequential. The five wells with As ≥ 10 µg/L gave HQ > 1 and carcinogenic risks above 10^{-4} although they comply with the national limit of 50 µg/L. Given that arsenic is widespread in the alkaline unconfined aquifers of the Indus basin (Podgorski et al., 2017; Younas et al., 2025) and is a global groundwater threat (Podgorski & Berg, 2020), these results support aligning the national standard with the WHO guideline of 10 µg/L. Sodium, which the HQ framework ignores, is a further concern: drinking water alone supplied up to 122% of the WHO daily limit before any food intake. In view of the evidence linking saline drinking water to raised blood pressure in coastal populations (Khan et al., 2011; Scheelbeek et al., 2017; Naser et al., 2019; Mueller et al., 2024), sodium should be treated as a health parameter rather than an aesthetic one in the Indus Delta.

The intervention classes in Table 7 translate into a three-tier response. In the saline zone (cluster C3 and SMI > 1), source substitution through canal-fed treatment, rainwater harvesting or community reverse osmosis is needed. In the fluoride hot spots of Sirani, defluoridation or blending should be prioritised for households with young children. Across all UCs, wellhead upgrading combined with turbidity-triggered bacteriological surveillance would address the faecal hazard. These measures sit

within the wider need to strengthen groundwater governance and drinking-water monitoring in Pakistan (Qureshi, 2020; Fida et al., 2023; Ali et al., 2024).

5.6 Comparison with other coastal and shallow aquifers

Placed alongside recent work from other coastal and shallow aquifers in South Asia and China (Table 8), the Badin results are moderate in salinity but distinctive in structure. The proportion of wells with SMI > 1 (23.7%) is less than half that reported for 1228 wells along the east coast of India (Sarkar et al., 2026), consistent with the inland position of the sampled villages and the small seawater fractions estimated here. The prevalence of *E. coli* (23.7%) lies within the 19–64% range observed month to month in shallow Bangladeshi tubewells (van Geen et al., 2011) and below the 41% reported for 902 tubewells by Ercumen et al. (2017), and fluoride-driven probabilistic risk resembles that reported for coastal Bangladesh (Rahman et al., 2020) and the west coast of India (Agarwal & Dhakate, 2024). What distinguishes the present study is not the magnitude of any single hazard but the joint, well-level test of their independence and its translation into intervention classes, which none of these studies attempted. Because faecal indicators are imperfect proxies for pathogens (Ferguson et al., 2012), the wellhead classes should be interpreted as indicator-based screening rather than direct pathogen risk.

The relevance of these results extends well beyond Badin. Subsiding, sediment-starved deltas such as the Ganges–Brahmaputra, Mekong and Nile host some of the world's densest rural populations relying on shallow hand pumps (Syvitski et al., 2009), and saltwater intrusion is expected to expand the number of people drinking saline groundwater by 2050 (Mueller et al., 2024). Recent basin- and coast-scale assessments in the Ganga basin and coastal China likewise report salinity-driven water types alongside significant health risks (fluoride and nitrate for children in the Ganga basin; arsenic and heavy metals on the Chinese coast), but evaluate the chemical hazards alone (Li et al., 2025; Raicy et al., 2026). Faecal contamination of supposedly improved sources is equally widespread in low- and middle-income countries (Bain et al., 2014) and rises in the wet season (Kostyla et al., 2015). Where both hazards co-exist, the decoupling test applied here (cross-tabulating a salinity flag against *E. coli* and regressing *E. coli* on turbidity, depth and recharge-borne solutes) requires only parameters already measured in routine monitoring, and the resulting intervention classes can be generated without additional fieldwork. The approach therefore offers water agencies in other coastal deltas a low-cost way to separate sources that need aquifer-scale solutions from those that can be fixed at the pump, and to avoid investing in treatment where repairing the wellhead would suffice.

Table 8. Comparison of the present results with recent studies of coastal and shallow drinking-water aquifers in South Asia and China.

Study	Setting (sample size)	Salinity and geochemistry	Microbial and health findings
This study	Lower Indus Delta, Pakistan (93 hand pumps)	SMI > 1 in 23.7%; seawater fraction ≤ 15%; evaporation and cation exchange dominate	*E. coli* in 23.7%, independent of salinity; Monte Carlo child HI > 1 in 46%
Sarkar et al. (2026)	East coast of India (1228 wells)	SMI > 1 in 55%; 39% saline by facies evolution diagram	–
Agarwal and Dhakate (2024)	West coast of India (57 wells)	Seawater influence; reverse ion exchange	Nitrate and fluoride hazard index above limits
Rahman et al. (2020)	Coastal Bangladesh	–	Probabilistic fluoride risk in drinking water
Ercumen et al. (2017)	Rural Bangladesh (902 shallow tubewells)	–	*E. coli* in 41%; sanitary scores not predictive
van Geen et al. (2011)	Bangladesh (125 shallow tubewells)	–	*E. coli* in 19–64% of wells per month; inversely related to arsenic
Knappett et al. (2012)	Bangladesh (shallow tubewells)	–	Unsealed wells contaminated more often than sealed wells
Raicy et al. (2026)	Ganga River Basin, India (3417 wells)	Salinity-driven Na–Cl zones in western and deltaic regions; EWQI	Child HQ > 1 for nitrate in 28% and fluoride in 25% of locations (Monte Carlo)
Li et al. (2025)	Coastal plain, Pinghu, China (seasonal)	Seawater intrusion; EWQI up to 191 at affected wells	As, Cd and Cr main carcinogenic risks; seasonal shifts
Ullah et al. (2026)	Dadu canal command, Sindh, Pakistan	F^- 0.5–6.35 mg/L; As 0.5–22 µg/L; rock–water interaction	F^-–As co-contamination mapped with machine learning

5.7 Limitations

The dataset comes from a single campaign, so seasonal changes in salinity and microbial loads are not resolved. SMI thresholds were set at the 75th percentile rather than derived from cumulative-probability inflection points, and saturation indices were computed without full ion-pair speciation. The risk assessment covered ingestion only and used default exposure factors; actual water intake is probably higher in this hot climate. Repeat pre- and post-monsoon sampling, Br^-/Cl^- ratios and stable isotopes would help separate modern seawater from relict marine water and drainage effluent,

and structured sanitary surveys would allow the wellhead pathways identified here to be quantified directly.

6. Conclusions

Drinking-water risk in the shallow coastal aquifer of Badin consists of two statistically independent hazards acting at different scales: an aquifer-scale geogenic hazard and a wellhead-scale faecal hazard. Recognising this decoupling, rather than reporting an aggregate proportion of unsafe wells, is the key to choosing interventions that work.

Shallow hand-pump groundwater in the Badin and Shaheed Fazul Rahoo talukas is predominantly of Ca–Mg–Cl–SO_4 and Na–Cl–SO_4 type, and TDS, Cl^-, hardness and Na^+ exceed drinking-water guidelines in 42–58% of wells. Salinity is governed by a single integrated factor combining evaporative concentration, direct and reverse cation exchange and marine mixing; marine mixing affects about one-quarter of wells, mainly in Sirani, at seawater fractions below 15%.

The weighted-arithmetic WQI is structurally biased towards fluoride and turbidity and largely insensitive to salinity, whereas the entropy-weighted index ranks wells consistently with their hydrochemistry and classes half of them as medium to extremely poor. *E. coli* contamination (23.7% of wells) is decoupled from aquifer chemistry and associated with turbidity, identifying wellhead ingress as the dominant pathway and turbidity as a practical screening indicator.

Probabilistic hazard indices exceed unity for 46% of child and 24% of adult exposures, mainly because of fluoride; a few wells carry carcinogenic arsenic risk despite meeting the national limit, and drinking-water sodium adds a cardiovascular risk not captured by standard indices. Only 26.9% of wells are free of all four hazards; 49.5% require treatment or a new source, 8.6% only wellhead repair and 15.1% both. Salinity and fluoride therefore require aquifer-scale or treatment-based solutions, whereas the faecal hazard can be removed cheaply at each pump. Seasonal monitoring, isotopic source tracing and alignment of the national arsenic standard with the WHO guideline are recommended next steps.

Acknowledgements

The authors thank the staff of the PCRWR Water Quality Laboratory, Badin, for analytical support and the residents of Gharo, Kadi Kazia and Sirani for access to their hand pumps.

Statements and Declarations

Funding

The authors declare that no funds, grants or other support were received during the preparation of this manuscript.

Competing interests

The authors have no relevant financial or non-financial interests to disclose.

Author contributions

Tarique Mahmood Noonari: Conceptualisation, Investigation, Resources, Data curation, Writing – original draft. **Nadeem Gul:** Methodology, Formal analysis, Software, Visualisation, Supervision, Writing – review & editing. **Sawera:** Investigation, Validation, Writing – review & editing. **Yousra:** Data curation, Software, Visualisation, Writing – review & editing.

Data availability

The data that support the findings of this study are available from the corresponding author upon reasonable request.

Ethics approval

Not applicable. The study involved no human participants or animals; water samples were collected from community and household hand pumps with the permission of their owners.

References

Adimalla, N., & Li, P. (2019). Occurrence, health risks, and geochemical mechanisms of fluoride and nitrate in groundwater of the rock-dominant semi-arid region, Telangana State, India. *Human and Ecological Risk Assessment*, *25*, 81–103. https://doi.org/10.1080/10807039.2018.1480353

Aeman, H., Shu, H., Abbas, S., Aisha, H., & Usman, M. (2023). Sinking delta: quantifying the impacts of saltwater intrusion in the Indus Delta of Pakistan. *Science of the Total Environment*, *880*, 163356. https://doi.org/10.1016/j.scitotenv.2023.163356

Agarwal, A., & Dhakate, R. (2024). Quality and health impact of groundwater in a coastal region: a case study from west coast of southern India. *Environmental Science and Pollution Research*, *31*, 56272–56294. https://doi.org/10.1007/s11356-024-34930-2

Alamgir, A., Khan, M. A., Schilling, J., Shaukat, S. S., & Shahab, S. (2016). Assessment of groundwater quality in the coastal area of Sindh province, Pakistan. *Environmental Monitoring and Assessment*, *188*, 78. https://doi.org/10.1007/s10661-015-5061-x

Ali, J., Noonari, T. M., Katohar, N. A., Jatoi, W. B., Jakhrani, M. A., & Hussain, K. (2024). Evaluation of physicochemical and bacteriological parameters in drinking water of the Badin district in Sindh, Pakistan. *Water, Air, & Soil Pollution*, *235*, 694. https://doi.org/10.1007/s11270-024-07510-w

Amiri, V., Rezaei, M., & Sohrabi, N. (2014). Groundwater quality assessment using entropy weighted water quality index (EWQI) in Lenjanat, Iran. *Environmental Earth Sciences*, *72*, 3479–3490. https://doi.org/10.1007/s12665-014-3255-0

APHA. (2012). Standard Methods for the Examination of Water and Wastewater, 22nd ed. American Public Health Association, American Water Works Association, Water Environment Federation, Washington, DC.

Bagordo, F., Brigida, S., Grassi, T., Caputo, M. C., Apollonio, F., De Carlo, L., Savino, A. F., Triggiano, F., Turturro, A. C., De Donno, A., Montagna, M. T., & De Giglio, O. (2024). Factors influencing microbial contamination of groundwater: a systematic review of field-scale studies. *Microorganisms*, *12*(5), 913. https://doi.org/10.3390/microorganisms12050913

Bain, R., Cronk, R., Wright, J., Yang, H., Slaymaker, T., & Bartram, J. (2014). Fecal contamination of drinking-water in low- and middle-income countries: a systematic review and meta-analysis. *PLoS Medicine*, *11*, e1001644. https://doi.org/10.1371/journal.pmed.1001644

Brown, R. M., McClelland, N. I., Deininger, R. A., & Tozer, R. G. (1970). A water quality index – do we dare? *Water and Sewage Works*, *117*, 339–343.

Du, J., Jia, C., Ding, Y., Yang, X., Feng, K., & Wei, M. (2025). Advancing wetland groundwater pollution zoning: a novel integration of Monte Carlo health risk modeling and machine learning. *Journal of Hazardous Materials*, *494*, 138412. https://doi.org/10.1016/j.jhazmat.2025.138412

Ercumen, A., Naser, A. M., Arnold, B. F., Unicomb, L., Colford, J. M., & Luby, S. P. (2017). Can sanitary inspection surveys predict risk of microbiological contamination of groundwater sources? Evidence from shallow tubewells in rural Bangladesh. *American Journal of Tropical Medicine and Hygiene*, *96*, 561–568. https://doi.org/10.4269/ajtmh.16-0489

Ferguson, A. S., Mailloux, B. J., Ahmed, K. M., van Geen, A., McKay, L. D., & Culligan, P. J. (2011). Hand-pumps as reservoirs for microbial contamination of well water. *Journal of Water and Health*, *9*, 708–717. https://doi.org/10.2166/wh.2011.106

Ferguson, A. S., Layton, A. C., Mailloux, B. J., Culligan, P. J., Williams, D. E., Smartt, A. E., Sayler, G. S., Feighery, J., McKay, L. D., Knappett, P. S. K., et al. (2012). Comparison of fecal indicators with pathogenic bacteria and rotavirus in groundwater. *Science of the Total Environment*, *431*, 314–322. https://doi.org/10.1016/j.scitotenv.2012.05.060

Ferguson, G., & Gleeson, T. (2012). Vulnerability of coastal aquifers to groundwater use and climate change. *Nature Climate Change*, *2*, 342–345. https://doi.org/10.1038/nclimate1413

Fida, M., Li, P., Wang, Y., Alam, S. M. K., & Nsabimana, A. (2023). Water contamination and human health risks in Pakistan: a review. *Exposure and Health*, *15*, 619–639. https://doi.org/10.1007/s12403-022-00512-1

Fisher, R. S., & Mullican, W. F. (1997). Hydrochemical evolution of sodium-sulfate and sodium-chloride groundwater beneath the northern Chihuahuan Desert, Trans-Pecos, Texas, USA. *Hydrogeology Journal*, *5*, 4–16. https://doi.org/10.1007/s100400050102

Gibbs, R. J. (1970). Mechanisms controlling world water chemistry. *Science*, *170*, 1088–1090. https://doi.org/10.1126/science.170.3962.1088

Giosan, L., Constantinescu, S., Clift, P. D., Tabrez, A. R., Danish, M., & Inam, A. (2006). Recent morphodynamics of the Indus delta shore and shelf. *Continental Shelf Research*, *26*, 1668–1684. https://doi.org/10.1016/j.csr.2006.05.009

Goswami, S., & Rai, A. K. (2025). Dynamics of fresh and saline groundwater interaction in coastal aquifers: a case study from the east coast, India. *Environmental Earth Sciences*, *84*, 516. https://doi.org/10.1007/s12665-025-12488-7

Güler, C., Thyne, G. D., McCray, J. E., & Turner, A. K. (2002). Evaluation of graphical and multivariate statistical methods for classification of water chemistry data. *Hydrogeology Journal*, *10*, 455–474. https://doi.org/10.1007/s10040-002-0196-6

Kaiser, H. F. (1958). The varimax criterion for analytic rotation in factor analysis. *Psychometrika*, *23*, 187–200. https://doi.org/10.1007/BF02289233

Khan, A. E., Ireson, A., Kovats, S., Mojumder, S. K., Khusru, A., Rahman, A., & Vineis, P. (2011). Drinking water salinity and maternal health in coastal Bangladesh: implications of climate change. *Environmental Health Perspectives*, *119*, 1328–1332. https://doi.org/10.1289/ehp.1002804

Knappett, P. S. K., McKay, L. D., Layton, A., Williams, D. E., Alam, M. J., Mailloux, B. J., Ferguson, A. S., Culligan, P. J., Serre, M. L., Emch, M., Ahmed, K. M., Sayler, G. S., & van Geen, A. (2012). Unsealed tubewells lead to increased fecal contamination of drinking water. *Journal of Water and Health*, *10*, 565–578. https://doi.org/10.2166/wh.2012.102

Kostyla, C., Bain, R., Cronk, R., & Bartram, J. (2015). Seasonal variation of fecal contamination in drinking water sources in developing countries: a systematic review. *Science of the Total Environment*, *514*, 333–343. https://doi.org/10.1016/j.scitotenv.2015.01.018

Li, P., Qian, H., & Wu, J. (2010). Groundwater quality assessment based on improved water quality index in Pengyang County, Ningxia, northwest China. *E-Journal of Chemistry*, *7*, S209–S216. https://doi.org/10.1155/2010/451304

Li, Z., Lu, C., Zhang, Y., Yu, X., Gao, Q., Yuan, Z., Wu, C., Liu, B., & Shu, L. (2025). Seasonal groundwater variations in the coastal plain under intense human activities: hydrochemical evolution, quality degradation, and health risk assessment. *Journal of Environmental Management*, *388*, 126062. https://doi.org/10.1016/j.jenvman.2025.126062

Mondal, N. C., Singh, V. P., Singh, V. S., & Saxena, V. K. (2010). Determining the interaction between groundwater and saline water through groundwater major ions chemistry. *Journal of Hydrology*, *388*, 100–111. https://doi.org/10.1016/j.jhydrol.2010.04.032

Mueller, W., Zamrsky, D., Oude Essink, G., Fleming, L. E., Deshpande, A., Makris, K. C., et al. (2024). Saltwater intrusion and human health risks for coastal populations under 2050 climate scenarios. *Scientific Reports*, *14*, 15881. https://doi.org/10.1038/s41598-024-66956-4

Naser, A. M., Rahman, M., Unicomb, L., Doza, S., Gazi, M. S., Alam, G. R., et al. (2019). Drinking water salinity, urinary macro-mineral excretions, and blood pressure in the southwest coastal population of Bangladesh. *Journal of the American Heart Association*, *8*, e012007. https://doi.org/10.1161/JAHA.119.012007

Natishah, A. J., Samuel, M. S., Velmurugan, K., Showparnickaa, S. R., Indumathi, S. M., & Kumar, M. (2025). Contamination of groundwater by microorganisms and risk management: conceptual model, existing data, and challenges. *Groundwater for Sustainable Development*, *29*, 101408. https://doi.org/10.1016/j.gsd.2025.101408

Pak-EPA. (2008). National Standards for Drinking Water Quality. Pakistan Environmental Protection Agency, Ministry of Environment, Government of Pakistan, Islamabad.

Park, S. C., Yun, S. T., Chae, G. T., Yoo, I. S., Shin, K. S., Heo, C. H., & Lee, S. K. (2005). Regional hydrochemical study on salinization of coastal aquifers, western coastal area of South Korea. *Journal of Hydrology*, *313*, 182–194. https://doi.org/10.1016/j.jhydrol.2005.03.001

Piper, A. M. (1944). A graphic procedure in the geochemical interpretation of water-analyses. *Transactions, American Geophysical Union*, *25*, 914–928. https://doi.org/10.1029/TR025i006p00914

Podgorski, J. E., Eqani, S. A. M. A. S., Khanam, T., Ullah, R., Shen, H., & Berg, M. (2017). Extensive arsenic contamination in high-pH unconfined aquifers in the Indus Valley. *Science Advances*, *3*, e1700935. https://doi.org/10.1126/sciadv.1700935

Podgorski, J., & Berg, M. (2020). Global threat of arsenic in groundwater. *Science*, *368*, 845–850. https://doi.org/10.1126/science.aba1510

Prüss-Ustün, A., Wolf, J., Bartram, J., Clasen, T., Cumming, O., Freeman, M. C., et al. (2019). Burden of disease from inadequate water, sanitation and hygiene for selected adverse health outcomes: an updated analysis with a focus on low- and middle-income countries. *International Journal of Hygiene and Environmental Health*, *222*, 765–777. https://doi.org/10.1016/j.ijheh.2019.05.004

Qureshi, A. S. (2020). Groundwater governance in Pakistan: from colossal development to neglected management. *Water*, *12*, 3017. https://doi.org/10.3390/w12113017

Rahman, M. M., Bodrud-Doza, M., Siddiqua, M. T., Zahid, A., & Islam, A. R. M. T. (2020). Spatiotemporal distribution of fluoride in drinking water and associated probabilistic human health risk appraisal in the coastal region, Bangladesh. *Science of the Total Environment*, *724*, 138316. https://doi.org/10.1016/j.scitotenv.2020.138316

Raicy, M. C., Aju, C. D., & Achu, A. L. (2026). Groundwater quality and risk in the Ganga River Basin: an integrated machine learning appraisal. *Environmental Geochemistry and Health*, *48*, 72. https://doi.org/10.1007/s10653-025-02964-1

Revelle, R. (1941). Criteria for recognition of sea water in ground-waters. *Transactions, American Geophysical Union*, *22*, 593–597. https://doi.org/10.1029/TR022i003p00593

Sarkar, B., Islam, A., Kumar, A., Talukdar, S., Sarif, M. N., Pandey, A., Lahiri, K., Mukherjee, S., Rahman, A., Haque, S. M., & Rahaman, A. (2026). Characterizing seawater intrusion and groundwater vulnerability to salinization along the east coast of India. *Journal of Contaminant Hydrology*, *277*, 104829. https://doi.org/10.1016/j.jconhyd.2025.104829

Scheelbeek, P. F. D., Chowdhury, M. A. H., Haines, A., Alam, D. S., Hoque, M. A., Butler, A. P., et al. (2017). Drinking water salinity and raised blood pressure: evidence from a cohort study in coastal Bangladesh. *Environmental Health Perspectives*, *125*, 057007. https://doi.org/10.1289/EHP659

Schoeller, H. (1965). Qualitative evaluation of groundwater resources. In: Methods and Techniques of Groundwater Investigations and Development. Water Resources Series No. 33, UNESCO, Paris, pp. 54–83.

Solangi, G. S., Siyal, A. A., Babar, M. M., & Siyal, P. (2019a). Application of water quality index, synthetic pollution index, and geospatial tools for the assessment of drinking water quality in the Indus Delta, Pakistan. *Environmental Monitoring and Assessment*, *191*, 731. https://doi.org/10.1007/s10661-019-7861-x

Solangi, G. S., Siyal, A. A., Babar, M. M., & Siyal, P. (2020). Groundwater quality evaluation using the water quality index (WQI), the synthetic pollution index (SPI), and geospatial tools: a case study of Sujawal district, Pakistan. *Human and Ecological Risk Assessment*, *26*, 1529–1549. https://doi.org/10.1080/10807039.2019.1588099

Syvitski, J. P. M., Kettner, A. J., Overeem, I., Hutton, E. W. H., Hannon, M. T., Brakenridge, G. R., et al. (2009). Sinking deltas due to human activities. *Nature Geoscience*, *2*, 681–686. https://doi.org/10.1038/ngeo629

Talpur, S. A., Noonari, T. M., Rashid, A., Ahmed, A., Jat Baloch, M. Y., Talpur, H. A., & Soomro, M. H. (2020). Hydrogeochemical signatures and suitability assessment of groundwater with elevated fluoride in unconfined aquifers Badin district, Sindh, Pakistan. *SN Applied Sciences*, *2*, 1038. https://doi.org/10.1007/s42452-020-2821-1

Uddin, M. G., Nash, S., & Olbert, A. I. (2021). A review of water quality index models and their use for assessing surface water quality. *Ecological Indicators*, *122*, 107218. https://doi.org/10.1016/j.ecolind.2020.107218

Ullah, Z., Ali, W., Ullah, I., Ahmad, T., Arslan, S., Rauf, S., & Licheng, P. (2026). Integrated machine learning and geochemical modeling reveal hydrogeochemical controls on fluoride and arsenic co-contamination in groundwater. *Environmental Geochemistry and Health*, *48*, 291. https://doi.org/10.1007/s10653-026-03161-4

Ullah, Z., Ullah, I., & Ali, W. (2025). Fluoride contamination and human health risks assessment in groundwater from community tube wells in Kamber Shahdadkot, Sindh, Pakistan. *Environmental Geochemistry and Health*, *47*, 474. https://doi.org/10.1007/s10653-025-02795-0

USEPA. (1989). Risk Assessment Guidance for Superfund, Vol. I: Human Health Evaluation Manual (Part A). EPA/540/1-89/002. U.S. Environmental Protection Agency, Washington, DC.

van Geen, A., Ahmed, K. M., Akita, Y., Alam, M. J., Culligan, P. J., Emch, M., et al. (2011). Fecal contamination of shallow tubewells in Bangladesh inversely related to arsenic. *Environmental Science & Technology*, *45*, 1199–1205. https://doi.org/10.1021/es103192b

Ward, J. H. (1963). Hierarchical grouping to optimize an objective function. *Journal of the American Statistical Association*, *58*, 236–244. https://doi.org/10.1080/01621459.1963.10500845

Ward, M. H., Jones, R. R., Brender, J. D., de Kok, T. M., Weyer, P. J., Nolan, B. T., Villanueva, C. M., & van Breda, S. G. (2018). Drinking water nitrate and human health: an updated review. *International Journal of Environmental Research and Public Health*, *15*, 1557. https://doi.org/10.3390/ijerph15071557

Werner, A. D., Bakker, M., Post, V. E. A., Vandenbohede, A., Lu, C., Ataie-Ashtiani, B., Simmons, C. T., & Barry, D. A. (2013). Seawater intrusion processes, investigation and management: recent advances and future challenges. *Advances in Water Resources*, *51*, 3–26. https://doi.org/10.1016/j.advwatres.2012.03.004

WHO. (2022). Guidelines for Drinking-Water Quality, 4th ed. incorporating the first and second addenda. World Health Organization, Geneva. https://www.who.int/publications/i/item/9789240045064

Yadav, S., & Kalkal, S. (2024). Health risk assessment using Monte-Carlo simulations due to arsenic contamination in groundwater in Punjab. *Journal of Water and Health*, *22*, 2304–2319. https://doi.org/10.2166/wh.2024.188

Younas, F., Sardar, M. F., Ullah, Z., Ali, J., Yu, X., Zhu, P., Guo, W., Al-Anazi, K. M., Farah, M. A., & Cui, Z. (2025). Assessment of groundwater chemistry to predict arsenic contamination from a canal commanded area: applications of different machine learning models. *Environmental Geochemistry and Health*, *47*(2), 46. https://doi.org/10.1007/s10653-024-02334-3